AD-A108 646 ADVANCED MECHANICAL TECHNOLOGY INC NEWTON MA F/G 11/2
HARD-ON-HARD (CERAMIC) LONG-LIFE SEALS AND RIDERS FOR CRYOGENIC--ETC(U)
AUG 81 F J CARIGNAN, A I WEST F33615-79-C-5029
UNCLASSIFIED AFWAL-TR-81-4060 NL

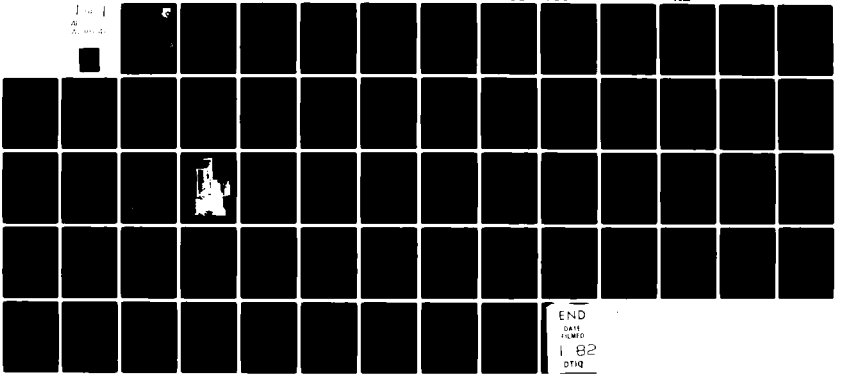

END
DATE FILMED
1 82
DTIC

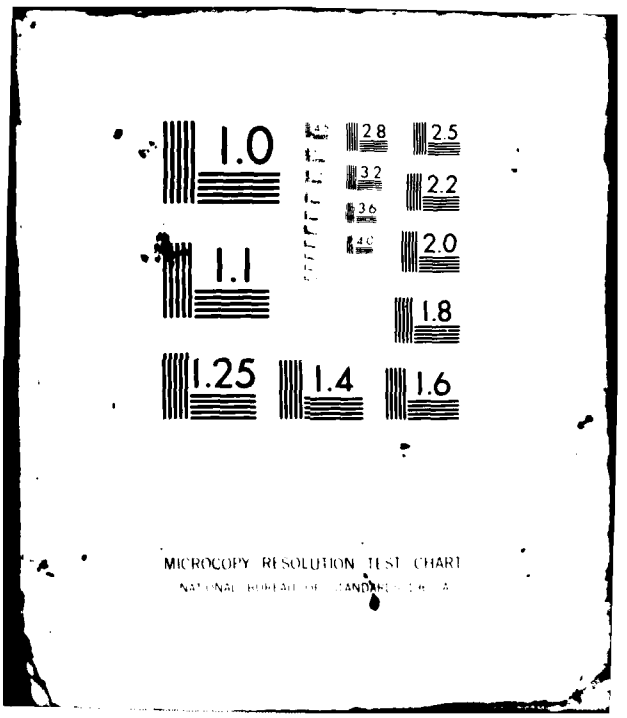
1.0
1.1
1.25
1.4
1.6
2.8
3.2
3.6
4.0
2.5
2.2
2.0
1.8
MICROCOPY RESOLUTION TEST CHART

AFWAL-TR-81-4060

HARD-ON-HARD (CERAMIC) LONG-LIFE SEALS AND RIDERS FOR CRYOGENIC COOLERS

Forest J. Carignan
Alan I. West

ADVANCED MECHANICAL TECHNOLOGY, INC.
141 California Street
Newton, Massachusetts 02158

August 1981

Final Report for June 1979 - October 1980

Approved for public release; distribution unlimited.

Materials Laboratory
Air Force Wright Aeronautical Laboratories
Wright-Patterson Air Force Base, Ohio 45433

NOTICE

When Government drawings, specifications, or other data are used for any purpose other than in connection with a definitely related Government procurement operation, the United States Government thereby incurs no responsibility for any obligation whatsoever; and the fact that the government may have formulated, furnished, or in any way supplied the said drawings, specifications, or other data, is not to be regarded by implication or otherwise as in any manner licensing the holder or any other person or corporation, or conveying any rights or permission to manufacture, use, or sell any patented invention that may in any way be related thereto.

This report has been reviewed by the Office of Public Affairs (ASD/PA) and is releasable to the National Technical Information Service (NTIS). At NTIS, it will be available to the general public, including foreign nations.

This technical report has been reviewed and is approved for publication.

Allan P. Katz

ALLAN P. KATZ
Project Engineer

Norman M. Geyer

NORMAN M. GEYER
Technical Manager
Processing and High Temperature
Materials Branch
Metals and Ceramics Division

FOR THE COMMANDER

Henry C. Graham

HENRY C. GRAHAM
Chief
Processing and High Temperature
Materials Branch
Metals and Ceramics Division

"If your address has changed, if you wish to be removed from our mailing list, or if the addressee is no longer employed by your organization please notify AFWAL/MLLM W-PAFB, OH 45433 to help us maintain a current mailing list".

Copies of this report should not be returned unless return is required by security considerations, contractual obligations, or notice on a specific document.

Unclassified

SECURITY CLASSIFICATION OF THIS PAGE (When Data Entered)

REPORT DOCUMENTATION PAGE		READ INSTRUCTIONS BEFORE COMPLETING FORM
1. REPORT NUMBER AFWAL-TR-81-4060	2. GOVT ACCESSION NO. AD-A103864	3. RECIPIENT'S CATALOG NUMBER
4. TITLE (and Subtitle) HARD-ON-HARD (CERAMIC) LONG-LIFE SEALS AND RIDERS FOR CRYOGENIC COOLERS		5. TYPE OF REPORT & PERIOD COVERED Final June 1979 - Oct 1980 6. PERFORMING ORG. REPORT NUMBER
7. AUTHOR(s) Forest J. Carignan Alan I. West		8. CONTRACT OR GRANT NUMBER(s) F33615-79-C-5029
9. PERFORMING ORGANIZATION NAME AND ADDRESS Advanced Mechanical Technology, Inc. 141 California Street Newton, Massachusetts 02158		10. PROGRAM ELEMENT, PROJECT, TASK AREA & WORK UNIT NUMBERS 24020424
11. CONTROLLING OFFICE NAME AND ADDRESS Materials Laboratory (AFWAL/MLLM) Air Force Wright Aeronautical Laboratories Wright-Patterson AFB, Ohio 45433		12. REPORT DATE August 1981 13. NUMBER OF PAGES 54
14. MONITORING AGENCY NAME & ADDRESS(if different from Controlling Office)		15. SECURITY CLASS. (of this report) Unclassified 15a. DECLASSIFICATION/DOWNGRADING SCHEDULE

16. DISTRIBUTION STATEMENT (of this Report)

Approved for public release, distribution unlimited.

17. DISTRIBUTION STATEMENT (of the abstract entered in Block 20, if different from Report)

18. SUPPLEMENTARY NOTES

19. KEY WORDS (Continue on reverse side if necessary and identify by block number)

Cryogenics, Tribology, Ceramics, Friction, Wear

20. ABSTRACT (Continue on reverse side if necessary and identify by block number)

A reciprocating pin-on-plate apparatus was designed and constructed for the testing of friction and wear characteristics of ceramic materials. The machine was specifically constructed to conduct tests at cryogenic temperatures in a pressurized (300 psig maximum) helium atmosphere. Cryogenic testing was not accomplished, but 17 ceramic materials were screened at room temperature in 15 psig helium. As a result of the screening tests, the materials were rank ordered according to their

DD FORM 1 JAN 73 1473 EDITION OF 1 NOV 65 IS OBSOLETE

Unclassified 294 236

SECURITY CLASSIFICATION OF THIS PAGE (When Data Entered)

20. (continued)

wear, and friction coefficients were tabulated. Several ceramics performed as well or better than fluorogold, a currently used seal material. Recommendations were made concerning additional materials to be tested and the materials characterizations needed for data analysis.

PREFACE

This report has been the result of efforts of a number of people. The authors wish to recognize contributions by the following individuals: Dr. Walter Syniuta, Dr. Lawrence Hoagland, Mr. Cyril Randall and Mr. Rolf Krischer.

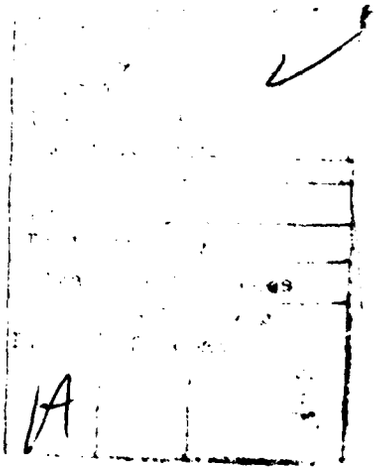

TABLE OF CONTENTS

LIST OF ILLUSTRATIONS

LIST OF TABLES

DEFINITION OF TERMS

A_1 = area of cold chamber, 2.5 ft^2

T_A = ambient temperature, 530^oR

T_C = cold chamber temperature, 60^oR

N = number of radiation shields

σ = Stefan-Boltzmann constant, 0.1713 x 10^{-8} $Btu/ft^2 \cdot hr \cdot R^4$

ΔT = 470^oR

F = view factor

ϵ = emissivity of radiating surfaces, estimate 0.1

S = stroke, 1 inch

D_c = average diameter of gap in drive tube, 0.9"

K_g = 0.07 $Btu/hr \cdot ft \cdot ^oR$, helium, average

K_{SS} = 6 $Btu/khr \cdot ft \cdot ^oR$, 304 stainless steel

g = gap between drive tube and containment tube, 0.032"

L = 11" shuttle tube length

L_L = 10.2", support leg length

SUMMARY

The life limiting factor in the existing cryogenic refrigerators for space applications is the wear of the polymeric seals and riders. Although there is interest in the use of ceramic materials for these seal and rider components, little data exists for the friction and wear characteristics of ceramics. Under this contract, a reciprocating pin-on-plate test apparatus was designed and constructed for the characterization of the friction and wear of materials. The apparatus is capable of operating in an environment of pressurized helium under a range of different loads and temperatures.

Pins and plates were prepared from a number of different ceramic and cermet materials, and a total of 18 one-hour screening tests were run at room temperature and 15 psig helium. The wear rates were determined both by mass and by volume loss of each pin, and the coefficient of friction was determined. A number of ceramics performed as well or better than fluorogold, a currently used seal material. These include hot pressed TiC, sintered Al_2O_3, siliconized SiC, hot pressed and reaction sintered SiC, and hot pressed B_4C. Recommendations were made concerning additional promising materials and the need to characterize each material in order to understand the wear rates reported.

SECTION I
INTRODUCTION

Vuilleumier cycle cryogenic refrigerators are being developed for space applications requiring high reliability and a long maintenance-free life of five years or more. These coolers are closed-cycle machines operating on high-purity helium as the working gas. To prevent performance deterioration from contaminant freeze-out in critical areas, it is essential to prevent the intrusion of gaseous and liquid contaminants into the working gas. Accordingly, use of liquid and/or grease-type lubricants is avoided and solid lubricants are used throughout these machines wherever sliding motion is encountered between adjacent parts. The most critical areas where solid lubricant materials limit service life are the displacer seals and riders employed on both hot and cold displacer assemblies. To date, the principal materials used for these components have been filled polymers such as Rulon, glass-filled TFE, polycarbonates and polyimides. Predicted life of these components based on extensive test and development work (AFFDL-TR-78-63) is still only 2-3 years, only half of the life goal.

Interest has developed in the possible use of hard ceramics for these seal and rider components in order to reach the life goals set for space-borne V-M refrigerators. However, very little data exists for the friction and wear characteristics of various ceramic materials combinations that might represent attractive candidates for this application. The objectives of this program were: (1) to develop a tribology test apparatus capable of operating in a pressurized helium environment over a range of temperatures and loads, and (2) to determine the friction and wear characteristics of candidate ceramics. A number of ceramic materials suited for use in seals operating at cryogenic temperatures were identified and screened at room temperature in helium.

SECTION II
FRICTION AND WEAR OF CERAMIC MATERIALS

Although the mechanical behavior of ceramics differs appreciably from metals, the classical theories of friction and wear can be useful in facilitating the selection of candidate materials as well as the interpretation of the test results.

1. FRICTION

Under normal circumstances, frictional force is directly proportional to the normal load and is independent of the apparent area of contact between the sliding surfaces and of the sliding speed. The proportionality of friction force and applied load is a consequence of the fact that each is equal to a material constant, characteristic of the surfaces in contact, multiplied by the same real area of contact. Since it is the real area of contact rather than the apparent area which governs the interactions between two sliding materials, and since the real area of contact is a function of the applied load and the material properties, friction force is independent of apparent area. Similarly, since the friction force depends upon the material properties and applied load, and since the strengths of most solids are only weakly dependent upon the rate of application of the stress, sliding velocity has only a weak effect on the friction force. In most cases where friction force appears to depend upon sliding velocity, this is usually explained by the fact that the local material properties have changed due to the higher interfacial temperatures experienced at high sliding speeds. Except for extremely smooth or extremely rough surfaces, friction is only weakly dependent on surface roughness, since most of the frictional work is done by inducing shear displacement of the junction interface.

In its simplest terms, the theory of sliding friction postulates that the real contact area between two sliding materials is proportional to the

applied load and inversely proportional to the resistance to plastic flow in compression (hardness of the weaker of the two materials in contact). Likewise, the resistance to shear displacement is proportional to the real area of contact and the resistance to plastic shear flow of the weaker of the two materials. Since the resistance of the weaker material to plastic flow in shear and in compression are related properties, it is not surprising to find that the ratio of these two quantities, and thus the friction coefficient, is quite similar for a wide range of materials.

Taking this simple theory one step further, it is reasonable that the shear resistance of the junction between two contacting materials will be affected by the degree of adhesion between the two materials. Indeed, it is found that for clean surfaces the friction coefficient increases with the ratio γ/H (surface energy of adhesion over hardness). Since ceramics tend to have low ratios of γ/H, typically an order of magnitude lower than for metals, they exhibit less adhesion, which is to the advantage of low friction. Like metals, in sliding friction of ceramic pairs or ceramic/metal pairs, the frictional properties tend to be those of the softer material and the nature of the harder material makes little difference. This is explained by the fact that the harder material tends to be covered by wear particles of the softer one, so that the junctions tend to contain the soft wear material alone.

There are significant examples of "non-ideal" behavior among certain nonmetals which can play an important role in reducing friction. Certain lattice-layer materials such as graphite, molybdenum disulfide, and cadmium iodide often exhibit low friction coefficients. Due to their layer-lattice structure, platelets detach themselves from the surface and are deposited on the surface of the (softer) metal with the result that sliding occurs between the harder layer-lattice material and its platelets, and the favorable frictional (and wear) properties of the layer-lattice material predominate over those of the metal. Some layer-lattice materials, such as graphite, exhibit this phenomenon only in the presence of water vapor or of some volatile organic material. Other materials, such as molybdenum disulfide, do not require such assistance. Conversely, some materials such

as boron nitride have a layer-lattice structure and a low surface energy, but are not especially good solid lubricants. They may, however, exhibit low friction properties compared with ceramics in general.

While the nature of the atmosphere surrounding metals in sliding contact may affect friction properties due to oxidation or surface contamination, the frictional properties of nonmetals are generally not similarly affected. Thus, little difference in frictional behavior of ceramics is expected when operated in air versus helium, except as the moisture content of atmospheric air may affect materials such as graphite.

2. WEAR

The two wear mechanisms that are likely to predominate in the sliding seals of the Hi-Cap cooler are adhesive and abrasive wear. There is a further possibility of brittle fracture wear for some materials having low tensile strengths relative to their compressive strengths.

a. Adhesive Wear

Adhesive wear is characterized by the transfer of material from one surface to another during sliding contact. It occurs because of strong adhesive forces that exist between atoms in intimate contact. Most experimental data obey the following relationship governing adhesive wear:

$$V = \frac{K \cdot L \cdot X}{3H}$$

where

V = volume worn away
X = distance slid
L = normal load
H = indentation hardness of worn material
K = wear coefficient

The wear coefficient K is the probability of forming a wear particle and is usually much smaller than 1. The value of K depends not only on the material itself but also upon the material on which is slides. Thus, K is a property of the material pair, not of the individual material. For a given sliding pair, existing data suggests that if two materials differ in hardness by a ratio R, their wear rates will vary inversely as R^2. Thus, with respect to adhesive wear, it does not appear that the wear of the harder material can be reduced to zero.

For a material of known hardness, K is the determining factor in rate of wear. While theoretical models exist for predicting K on the basis of material compatibility and surface energy of adhesion, these models are most applicable to rubbing metal surfaces and are not thought to be as applicable to ceramics or ceramic/metal pairs. The indentation hardness H of ceramic seals will probably change little from room temperature down to cryogenic temperatures, and K is not expected to change appreciably.

Another aspect of adhesive wear which affects the suitability of a candidate seal material is the maximum size of loose wear debris particles, which may plug the V-M cooler clearance seals or regenerators. Average loose particle diameter is related to material properties by the following equation(1):

$$D = \frac{60{,}000\gamma}{H}$$

where γ is the surface energy and H is the indentation hardness. Generally, no loose wear particles are formed which exceed the average diameter by more than a factor of 3. For a hard material such as Al_2O_3 with a value of γ/H of 0.34×10^{-8} cm, the average loose particle diamter is found to be approximately 2 microns. Thus, no loose wear particles formed via adhesive γ/H wear larger than about 6 microns would be expected. In contrast, steel would produce particles greater than 100 microns.

b. Abrasive Wear

There are two types of abrasive wear: Two-body and three-body abrasive wear. Two-body wear occurs when a hard, rough surface slides against a softer surface and plows grooves into it. Sandpapering or filing are examples. The second type arises when hard abrasive particles are introduced between sliding surfaces and material is abraded off each surface, as in lapping.

Abrasive wear is directly proportional to the applied load and sliding distance as in adhesive wear, but unlike adhesive wear, it does not exhibit a simple inverse proportionality to indentation hardness. A material which is only slightly harder than the material it is abrading will wear it away just as well as a much harder material would. Unlike adhesive wear, however, the harder material will experience insignificant abrasive wear.

Two-body abrasive wear can be eliminated if the harder sliding surface is smooth. Thus, a smooth ceramic against a rough steel shaft would cause no abrasive wear in either body since the softer steel will not cut the harder ceramic, and the smooth ceramic will not abrasively wear the softer steel. Since two-body abrasive wear can be effectively eliminated through appropriate geometric design of the sliding surfaces, two-body abrasive wear need not be a factor in seal design. However, in a sliding system, loose wear particles are formed via adhesive wear, and this wear debris may result in three-body abrasive wear. This too can become insignificant if the loose wear particles are small enough or soft enough.

c. Brittle Fracture Wear

The preceding discussions generally suggest the advantages of using brittle materials for sliding seals in the absence of lubrication, due to their characteristics of low wear rates and small loose debris particle sizes. Caution must be exercised, however, since brittle materials are subject to brittle fracture wear, which is characterized by series of cracks which form perpendicular to the wear track. Such cracks eventually lead to the formation of large wear particles produced as a result of

surface break-up, and can result in high rates of wear. In general, wear rates appear to be the highest for materials which have low values of tensile strength relative to their compressive strength. Materials whose tensile strength is less than 1/3 their compressive strength appear to be especially prone to this form of wear.(2)

In general, it is recognized that to obtain high hardness, high strength, and uniform flaw-free surface properties, it is desirable to obtain the finest grain size materials available which also have high density.(3) For most of these materials, this would be approximately 1 μm grain size with greater than 99% density from hot pressing. Recently, ceramists have recognized that for some materials, high fracture toughness (K_{IC}) can be obtained by proper control of microstructure or judicious additions of second phases. The most impressive materials presently available in this regard are hot pressed Si_3N_4 and partially stabilized ZrO_2 (with proper heat treatment) for which K_{IC} values of 10 MN/M^3 have been achieved.(4)

At present, mechanistic understanding of the friction and wear problem is relatively primitive. Much of the present theory is based on plastic behavior as exhibited in metals. For hard ceramics there are important differences. Plastic deformation will understandably occur locally at asperities or where foreign particles (or wear debris) can cause furrows to be cut. However, for hard ceramics, more elastic accommodation will occur because of the high yield stresses. In addition, material loss or surface damage will likely occur as a result of brittle crack propagation due to high contact stresses. This area is poorly understood, and has become the object of considerable recent study.(5,6,7) Much of the work has been on simple problems of indentation and its extension to multiple particle erosion. Although the problem of sliding friction is more difficult, the analyses of simpler problems may give some insight into the problems of contact stresses arising from surface asperities or from abrasion from foreign particles or wear debris. For a hard foreign particle, the response of the ceramic can be idealized as primarily elastic or primarily plastic depending upon the indenter (particle) shape and the total load. For spherical particles, the response will be primarily elastic and cone

cracks tend to form. If there are sufficient surface flaws, the critical load for forming a cone crack is:

$$P_c = \alpha_E r K_{IC}^2 / E \qquad (1)$$

where α_E depends on the elastic constants, r is the particle radius, K_{IC} is the fracture toughness ($\sqrt{2E\gamma}$), and E the sample modulus.[6] The final crack dimension, c will increase with load as:

$$P/c^{3/2} = \beta_E K_{IC} \quad (P > P_c) \qquad (2)$$

where the dimensionless constant β_E has not been quantitatively solved.

For a sharp indenter, the response is primarily plastic. In this case, medium (radial) cracks form on loading and lateral (parallel to the surface) cracks form on unloading. The critical load for median crack formation is:

$$P_c = \alpha_p K_{IC}^4 / H^3 \qquad (3)$$

where H is the hardness and α_p depends on elastic and plastic parameters. The crack size will depend on load as:

$$P/c^{3/2} = \beta_p K_{IC} \quad (P > P_c) \qquad (4)$$

where the dimensionless parameter β_p depends on the indenter shape. Generally, cracks will be larger and initiate under lower loads for the sharp indenter case. In both cases, if the surface has few defects, the critical loads will be greater than given by Eqs. (1) and (3). The results are more complicated for a sliding indenter and have not been analyzed in as much detail. For a spherical indenter, if the coefficient of friction exceeds 0.02, then the critical force law changes and P_c becomes proportional to r^2. Thus, these theories can only be used as a guide or starting point for more appropriate analyses.

It is seen that for all cases resistance to cracking will be greater for a high K_{IC} material. If cracks form, wear will eventually result from growth of lateral cracks to the surface or from connection of radial or cone cracks. The optimum values of E and H are less clear because high values may lead to lower friction, but also lower values of threshold loads for crack formation, Eqs. (1) and (3). Mass loss may also be less when the response is primarily elastic, thus favoring materials with high values of H/E.

In summary, ceramics appear to be especially well suited as materials for unlubricated sliding seals either as ceramic-on-ceramic or ceramic-on-metal. The physical properties which enhance their applicability are their low values of surface energy γ, and their high values of indentation hardness H. These properties lead to lower friction, low adhesive wear, low abrasive wear, and minimal loose debris particle size.

SECTION III
FRICTION AND WEAR APPLICATIONS FOR CERAMICS

Currently there are a large number of hard ceramics which can be fabricated or obtained commercially. The development of engineering ceramics has been spurred on primarily by the need for materials which retain reasonable mechanical properties at high temperatures - an example being the emphasis over the past ten years on high temperature turbine engine requirements. Little or no work has been done at low temperature. The number of such materials has increased significantly in the past decade as ceramists have learned to process these materials to high density and fine grain size. Further improvements are being made as a result of continuing efforts to improve uniformity and to eliminate processing flaws which limit the material's strength. Materials such as SiC, Si_3N_4, B_4C, and many oxides are either commercially available or readily obtained from specialty suppliers. Quite often, however, the mechanical properties of samples of chemically similar materials obtained from different suppliers are quite different.

Little or no information on the tribological behavior of monolithic ceramics, ceramic coatings or hard metallic coatings is available.[8,9] In certain high performance Diesel engines where scuffing of the top rings has been a problem, plasma-sprayed ring coatings of titanium carbide, chrome carbide, molybdenum, ceramics (alumina-titania-calcium fluoride, tungsten carbide, boron nitride-nichrome), and other high melting temperature materials have been successful in eliminating ring scuffing.

It has been shown that in prolonged sliding tests of silicon carbide on silicon nitride, a silicon layer develops on the surfaces, after which the friction and wear increases drastically. Therefore, this combination of ceramics may need to be avoided. A similar situation may also occur with silicon nitride on silicon nitride after longer periods of time when operating at high temperatures. Different material combinations may be required to get around this problem. A silicon layer does not develop when

sliding boron carbide and silicon nitride, and as a result, this may be a good material combination except for high temperature applications. However, the combination of hot pressed aluminum oxide sliding on silicon nitride does appear promising at high as well as low temperatures.

Godfrey, of the Admiralty Materials Lab in England, has done a great deal to promote the use of ceramics in conventional internal combustion engines. (8,10,11,12) He has successfully demonstrated the operation of a reaction bonded silicon nitride (RBSN) ceramic piston, rings and piston pin in a 2 HP Villers 4-stroke single cylinder gasoline engine. Two sets of triple segment RBSN rings were fitted on metal backing springs in the piston grooves, the rings being segmented to avoid fracturing the rings on installation. Godfrey has also demonstrated the use of a RBSN piston and rings in a single cylinder 4-stroke water-cooled Gardner IL2 Diesel engine of 108 mm bore and 152.4 mm stroke which develops 12 HP.

Norton Company demonstrated the superior wear resistance of ceramic reciprocating engine cylinder liners nearly 20 years ago (unpublished).(13) During the early 1960's, some development work on wear resistant cylinder liners for internal combustion engines and for deep well oil pumps was conducted. This work was prompted by the relatively short wear life of alloy liners of some in-plant internal combustion engines, when used in factory areas having a high content of abrasive dust (e.g., foundries and parts for oil well and slurry pumps used in the mining industry). Hot and cold-pressed aluminum oxide ceramic cylinder liners were inserted in a metal sleeve in both Caterpillar and Waukesha engines, and tested with standard pistons and rings. No sign of wear was evident after operation of the engines under conditions which severely wore cast iron cylinders in the past.

In another test (unpublished) ceramic cylinder liners were used in a Briggs and Stratton air-cooled engine.(13) Liner wear, ring wear and oil consumption data is shown in Table 1, after operation at full load at 2000 RPM (approximate equivalent of 18,000 miles). In the three cases where ceramic liners were used, the test period was 600 hours versus 400 hours with a cast iron liner. However, in spite of the longer test, the ring wear

TABLE 1

TEST RESULTS - CERAMIC CYLINDER LINERS
BRIGGS-STRATTON AIR COOLED ENGINE

Cylinder Liner Material	Hours Run	Cylinder Finish (μ in.)	Cylinder Wear on Diameter	% Wt. Loss Ring Wear			Oil Consumption
				Top	Middle	Bottom	
Cast Iron	400	5 to 50	0.0007"	3.96	1.67	3.05	4200 CC
Al_2O_3 (LA29A)	600	30 to 50	0.0002"	1.64	0.74	1.41	1650
Al_2O_3 (LA162)	600	10 to 15	Not Measurable	1.61	0.56	0.97	1400
Hot Pressed B_4C	600	5 to 15	Not Measurable	1.33	0.45	0.68	1150

and oil consumption with ceramic liners were reduced to less than half, and cylinder liner wear was reduced to a negligible value. In one instance, a ceramic connecting rod bearing was used for a period of 200 hours, resulting in no measurable wear of the refractory; polishing of the alloy steel pin was the only evidence of running.

Other experimental work which is of interest is the experience of Ricardo Consulting Engineers, England.[13] Over the past 15 years, Ricardo have carried out a limited number of simple engine experiments to evaluate ceramic materials. These experiments were mainly aimed at assessing material compatability and durability and included:

- During the work carried out on wear rates in marine engines, tests were made with 70/30 alumina/nickel alunimide cermet sprayed in narrow bands on a V/Ti iron liner. This resulted in excessive ring and liner wear due to the cermet becoming detached and abrading.

- Three adjacent strips of alumina, chrome oxide and zirconia were sprayed onto the crown and skirt of an aluminum alloy piston of a gasoline engine. The coatings were 0.035 in. thick. After 10 hours running at full throttle at speeds up to 3000 rev/min, portions of the chrome oxide and zirconia had become detached.

These earlier attempts at using ceramics were generally disappointing, but the improved materials and techniques for coating now available can yield more tenacious coatings. More recently (1974), Syniuta et al applied zirconium oxide coatings (0.035") to steel piston crowns in a Rankine cycle expander operating with 1000°F/1000 psig steam.[14] Two pistons were coated and tested successfully in single cylinder engines at Scientific Energy Systems Corporation. Additionally, a high-pressure water pump piston was made from hot pressed silicon carbide, and was run in a pump pumping boiler water with no other lubricant at 1200 psi/230°F with no visible evidence of wear after seven hours of testing.

SECTION IV
CANDIDATE CERAMIC MATERIALS FOR LOW TEMPERATURE SEALS

1. SIGNIFICANT MATERIAL PROPERTIES

The material properties which are relevant to the selection of appropriate candidate ceramics for low temperature seals are Young's modulus E, fracture strength σ, thermal expansion coefficient α, hardness H, density ρ, surface energy γ, and fracture toughness K_{IC} at room temperature down to 11°K. Of lesser importance is the conductivity k, and slow thermal shock parameter $k\sigma/\alpha E$.

Plasticity theory dictates that the coefficient of friction $\mu \simeq \tau_y/H$, τ_y being the shear strength, and therefore μ ranges from 0.4 to 1 (from continuum theory). However, low values of γ/H are also needed to avoid adhesion. Obviously, adsorbed layers lower γ, but moisture or other species are not likely to be effective at the extremely low operating temperature indicated. If a material is strongly anisotropic and properly oriented, then τ_y/H will be low, as for graphite, MoS_2, BN and mica and can result in low friction. For sufficiently high values of H/E, the deformation may be primarily elastic, again resulting in lower friction.

Adhesive wear theory dictates ($V = KLX/3H$) that high hardness H should result in low wear volume. Additionally, a low γ/H will also lower the wear rate. All the materials being considered have high hardness, and therefore, adhesive wear may not be the limiting wear mechanism. Microcracking from contact stresses at asperities, foreign particles or wear debris may be the most important factor, and therefore, a high fracture toughness (K_{IC}) material would be desirable. A high H/E ratio material will provide better elastic compliance and decohesion on unloading and thus lower wear. In addition, the surface flaw sizes are expected to play a very important role - smaller pre-existent cracks would be expected to give longer "incubation" time before reaching critical growth size.

To obtain a uniform, flaw-free surface as well as high hardness and strength, a candidate material should possess a fine grain size The presence of porosity in sintered or plasma deposited material will give rise to stress concentrations and consequently reduce the material's fracture toughness.

In cermet materials, it is important that the ceramic particle size be small and the shape be smooth to reduce pullout and abrasive wear.

A candidate material should be homogeneous as to its phase content, and the phase distribution and impurity content should be consistent between material heats.

2. MATERIALS SELECTION

A number of ceramic suppliers were contacted as to the optimum choice of state-of-the-art materials as well as new and proprietary materials. The following is a list of manufacturers contacted:

AMMRC
Associated Engineering Developments
Atomergic Chemicals Corporation
AVCO Corporation
Carboloy
Carborundum Corporation
Ceradyne Inc.
Chemetal
Coors Porcelain Company
Corning Glass Works
Deposits & Composites, Inc.
General Electric Company
GTE-Sylvania, Inc.
Kawecki-Berylco Industries, Inc.
Kennametal
Koppers Company, Inc.
Kyocera
Man Labs, Inc.
Max Planck Institut
NTK
Norton Company
Perfect Circle (DANA Corporation)
Quad Group
Ramsey Corporation
Raytheon Company
Rockwell International Science Center
3M Company
Toshiba Corporation

Union Carbide Corporation
USAFWAL (WPAFB)
USNRL
United Technologies

Of all the ceramic materials available, the two leading materials for high temperature use are silicon carbide (SiC) and silicon nitride (Si_3N_4) due to their good thermal shock resistance, corrosion-erosion resistance, and mechanical properties. Of the two, silicon carbide is harder and has greater thermal conductivity. High density and strength can be achieved by hot pressing, reaction sintering, or solid-state sintering. On the other hand, silicon nitride has better strength and thermal shock resistance but should be fabricated by hot pressing as sintering or reaction sintering produces in this case a lower density, lower strength material.

Aluminum oxide (Al_2O_3) is another common ceramic exhibiting good compressive strength, plus chemical and abrasive resistance, and it can be polished to a high surface finish.

Titanium carbide is a ceramic material displaying excellent wear resistance and is currently used for cutting tools. It also has high flexural and compressive strength but also a high value of Young's modulus.

Boron carbide (B_4C) is one of the hardest of ceramic materials with excellent wear resistance and is capable of being polished to very fine surface finishes.

Zirconia (ZrO_2) has an extremely low thermal conductivity making it ideally suited for adiabatic diesel applications. It also can be heat treated to obtain optimum grain size and fracture toughness. Zirconia has been used in extrusion dies and is reported to have a low friction coefficient.

In addition to these monolithic ceramic materials, there are a number of ceramic composites, cermets, and plasma deposited materials of interest. An Al_2O_3-BN composite has been developed by U.S. Naval Resesarch Laboratory because of its excellent thermal shock characteristics, and at temperatures greater than 500°C an oxide of boron forms (B_2O_3) which appears to

strengthen further the material. Additionally, the boron nitride (hexagonal) is thought to give the composite lubricity while the alumina adds hardness and strength.

Los Alamos Scientific Laboratory produces a TaC-NbC material containing 40% graphite which should significantly lower the coefficient of friction in an environment containing moisture, but which may not be efficacious in a cold, dry atmosphere. Plasma sprayed and chemical vapor deposited materials have been developed that exhibit good adhesion to substrate materials. Zirconia and alumina have been sprayed onto piston crowns and cylinder liners and appear to withstand the thermal cycling well. Alumina-titania is routinely deposited onto piston rings for use in small internal combustion engines such as those produced by Briggs and Stratton. In 1979, Ramsey Corporation sold 750,000 of these ceramic coated piston rings.(15)

Chemical Vapor Deposition (CVD) is reported to produce a fully dense monolithic material. The major limiting factor is the requirement that the substrate material have the same thermal expansion coefficient. SiC can be deposited onto graphite or SiC, while WC can be successfully deposited onto tungsten. Chemetal is attempting to refine the process so as to allow the coating of steel while retaining good thermal shock resistance.

It has been difficult to characterize each material from information obtained from suppliers or the literature as there is no standard by which the materials have been tested. Hardnesses are reported in Vickers, Rockwell (A or N), and Knoop units, making conversions difficult. Likewise, the fracture toughness is reported via torsional tests or notched beam, and values of the Weibull modulus for many of these tests are not given. Grain size, porosity, and impurity content are not reported, and information regarding the sintering agents used and the exact chemistry is considered proprietary information. Compounding the issue of characterization is the variability of mechanical and physical properties between heats from the same supplier.

A wide range of representative ceramic materials were chosen for testing. Table 2 lists these with their material properties as reported by the suppliers.

TABLE 2

MATERIAL CHARACTERIZATIONS

MATERIAL	SUPPLIER	FABRICATION METHOD	DESIGNATION	ρ (g/cc)	% THEORETICAL ρ	σ_f MPa	E GPa	α $10^{-6}/^{\circ}C$	H MPa	K_{IC} $MN_m^{-3/2}$	k $W/M\cdot^{\circ}C$
Si_3N_4	AED	RS	Nitrasil	2.49	90.3	190	170	3.1	18.4	---	16.
B_4C	AVCO	HP	---	2.52	99.	346	470	4.3	24.1	6.0	30.
Sialon	AVCO	HP	---	--	--	475	---	---	--	5.0	--
AlN	Ceradyne	HP	137	3.13	96.	---	---	---	--	---	--
Pyroceram	Corning		9606	2.61	--	138	119	5.8	4.80	---	3.4
Al_2O_3	Kyocera	S	A473	3.6	89.3	317	269	6.5	9.30	---	19.6
Al_2O_3	Kyocera	S	A479	3.8	95.1	303	345	7.7	11.4	---	25.0
Si_3N_4	Kyocera	S	SN220	3.2	99.	490	296	3.7	12.5	4.1	12.6
TiC/Ni-Mo	Kennametal		K162B	6.1	--	1580	407	3.8	(89.5RA)	---	19.2
NbC-TaC-C	Los Alamos	HP	S-4181A	--	97.4	---	---	---	--	---	--
Si_3N_4	Norton	HP	NC132	3.2	99.5	800	325	3.2	18.4	4.5	32.
SiC	Norton	HP	NC203	3.2	99.8	441	441	4.3	20.6	4.5	81.
SiC-Si	Norton	RS	NC435	3.05	96.6	462	352	4.8	--	---	57.
SiC	NTK	RS	EC412	3.15	--	350	430	4.6	(91.6R45N)	---	77.
SiC	NTK	S	EC422	3.13	--	530	450	4.8	(93.0R45N)	---	65.
TiC	USAFWAL	HP	---	4.92	--	---	---	7.6	19.3	---	--

RS = REACTION SINTERED
HP = HOT PRESSED
S = SINTERED

SECTION V
FRICTION AND WEAR TEST APPARATUS

It is not practical to duplicate precisely the friction and wear conditions occurring in the Hi-Cap cooler, particularly during the initial screening test. If meaningful test data on many material pairs are to be obtained in a short period of time, accelerated testing must be performed under test conditions which retain their relevancy to the intended application. Such testing should duplicate the ambient conditions and magnitudes of loads and sliding velocities, but with small apparent contact areas. Excessive acceleration of wear testing tends to give invalid results due to secondary effects such as frictional heating and excessive plastic deformation. For the typical loads and surface speeds encountered in the Hi-Cap cooler, test loads no greater than 20 lbs, and speeds no greater than 600 strokes/minute (1" stroke) will permit accelerated wear testing without significant departures from the conditions characteristic of the Hi-Cap cooler.

To achieve these objectives, a reciprocating pin-on-plate friction and wear test apparatus capable of being operated in a helium environment at controlled temperatures over the desired range was designed and built. In this apparatus, a 1/4" diameter pin with a hemispherical end slides over a flat plate in reciprocating motion generated by a crank-connecting rod mechanism. This approximates the motion of the displacers in the Hi-Cap cooler.

A general assembly drawing of the test apparatus is shown in Figure 1 and a picture of the apparatus is shown in Figure 2.

The pin is held in a split sleeve which grips it firmly, but will not damage it as a direct set screw would. The pin reciprocates across the same wear track on the plate. The oscillatory linear motion is desirable for testing from a number of standpoints. For one, it simulates the reciprocating motion of the Hi-Cap cooler. Secondly, it provides in a single test wear

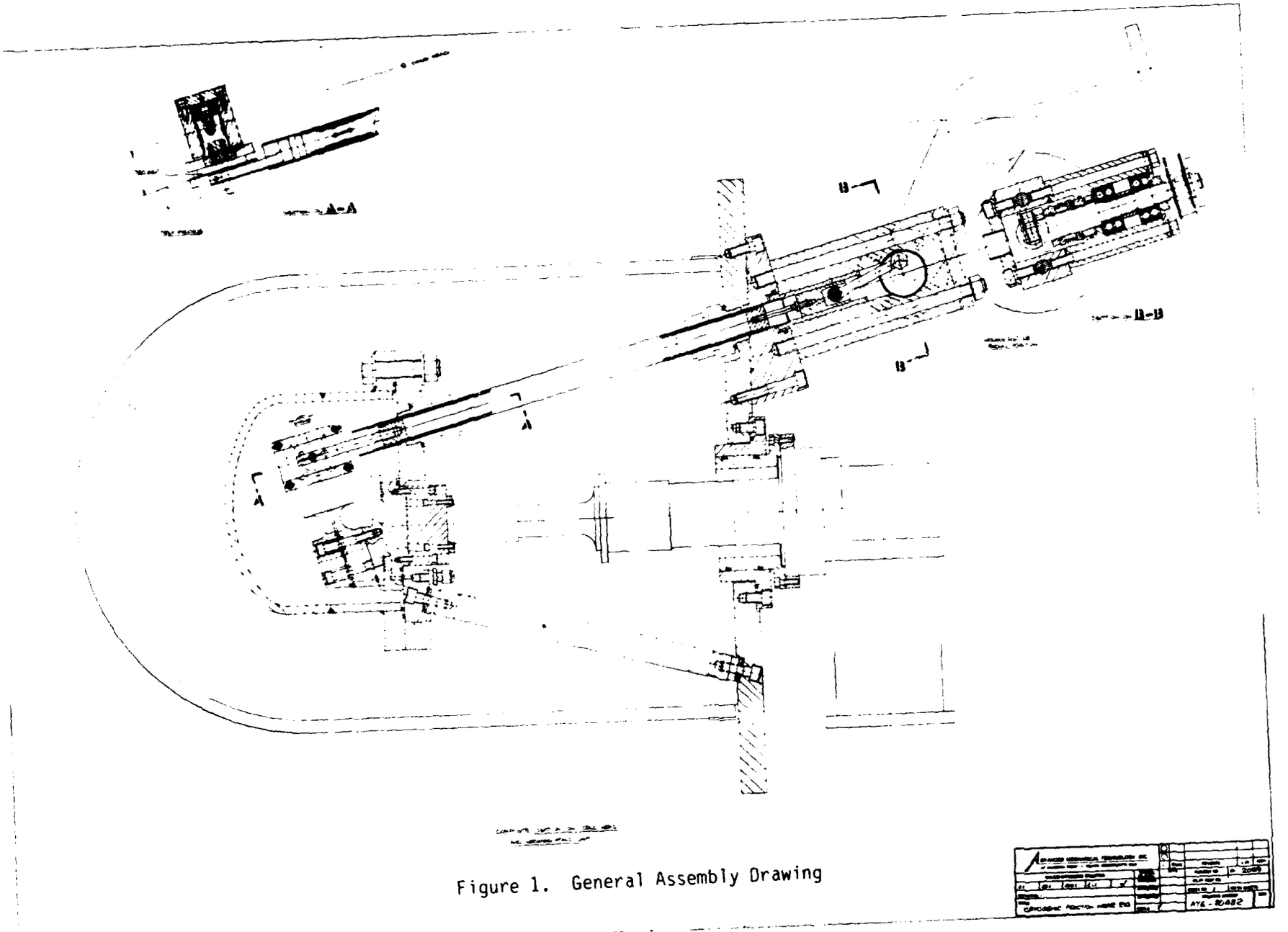

Figure 1. General Assembly Drawing

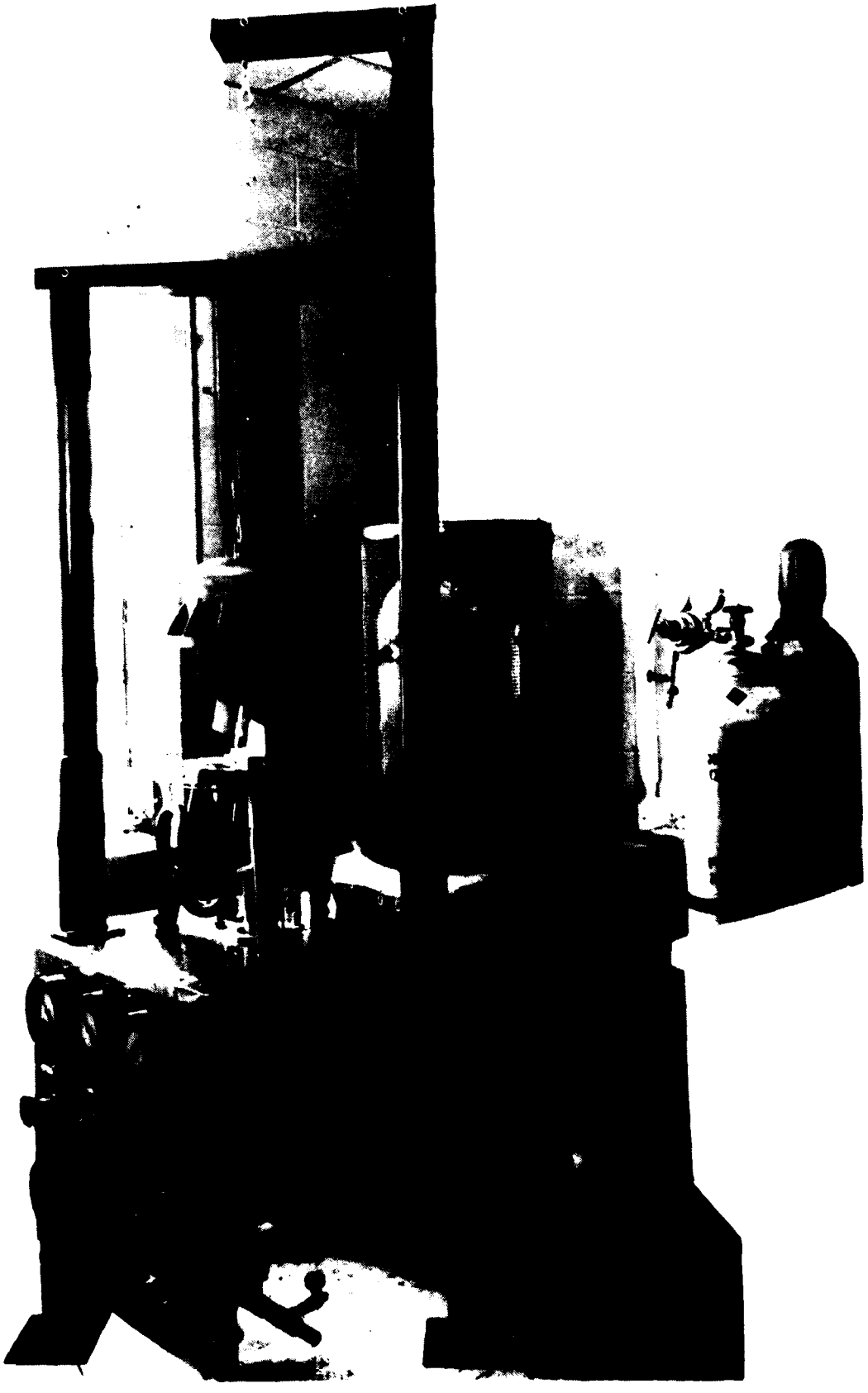

Figure 2. Photograph of Apparatus

rates and friction coefficients over a wide range of speeds. Profilometer traces of the wear track at different positions will give the wear rate at various sliding speeds, and specimen weight losses will give an average wear rate. The friction coefficient can be recorded continuously.

The principal features of the test apparatus are described below. The test chamber itself is built from an 8" stainless steel pipe cap with a special bolting flange and a mating baseplate. It will permit testing at 500 psi. All low temperature seals are metal O-rings. This high-pressure, low-temperature vessel is supported on three legs in an evacuated bell jar. A fourth leg enters the baseplate and encloses the reciprocating shaft which moves the pin specimen across the plate specimen. Practical operation of the test specimens at cryogenic temperatures requires that the whole pressurized assembly be run at the test temperature. This necessitates the use of the evacuated bell jar surrounding the pressurized test chamber in order to eliminate heat conduction through air. Several layers of aluminized mylar reduce radiation losses to an acceptable level, and the miscellaneous losses remaining are small enough to be tolerated. These include conduction along the legs and transfer tubes and also the shuttle loss due to the reciprocating shaft in the drive tube. These losses are estimated to be about 10 watts at 33°K.

The high pressure system was assembled with Vacuum Goop as a thread lubricant to prevent galling of stainless steel parts.

Cooling was to be provided by a CRYODYNE low temperature refrigeration unit. The CRYODYNE can provide 22 watts of cooling at 33°K. Most of the cooling load anticipated would be from the frictional heating. As a secondary means for cooling, liquid nitrogen can be run through coils brazed to a copper junction block located between the CRYODYNE cold head and the dynamometer base. Copper-constantan thermocouples were installed to monitor the temperature of the stainless steel pressure vessel baseplate and the temperature of the copper specimen mounting plate. These thermocouples would serve for all testing from room temperature to 77°K. For low temperature testing at 33°K, gold-iron thermocouples could be employed due to their greater sensitivity at 33°K. Thermocouple output signals would be

read on a digital millivoltmeter. Cartridge heaters are located in the baseplate to bring the system to room temperature rapidly after conducting a low temperature test.

1. DRIVE SYSTEM

The reciprocating motion for the test apparatus was to be provided by a contamination-free sealed linear motor. A prototype motor was built which had a stroke of one inch at speeds of up to 10 hertz. A second motor with theoretically improved performance was also built and installed in the test apparatus. The complete design of the motor is presented in the Appendix.

It was found that the second and final linear motor did not perform satisfactorily. Preliminary indications seemed promising but the second motor performed poorly. The motor had a low force output and a great deal of plunger heating. An in-depth analysis was not performed because time was important and an immediate solution was not apparent. Instead, an unlubricated crank-connecting rod arrangement was built and a tungsten carbide face seal used to isolate the clean high pressure helium system. The pressure differential across the seal is limited to 300 psi and the life of the unlubricated seal unknown. Generally, face seals are operated with a lubricant on at least one side of the seal. This is not a desired operating condition, and it was the basis behind developing the linear magnetic drive. The manufacturers of the face seal (Sealol) did not know how long the unlubricated seal would last, but life is projected to be in the hundreds of hours. The seal can be operated until the helium leakage is excessive.

The crank-connecting rod-type drive mechanism is mounted beneath the vacuum base plate. The crank, connecting rod, crosshead and the long reciprocating drive rod are all located inside the high pressure helium environment. All bearings and other sliding surfaces in this drive mechanism employ low outgassing type solid lubricated materials in order to eliminate the possibility of contaminating the test sample surfaces with unwanted lubricant films that are not present in the Hi-Cap cooler. Specifically,

these solid lubricant bearing surfaces utilize Feurlon C* bushings running against polished stainless steel surfaces. This material is similar to those currently employed in the Hi-Cap cooler.

2. PRESSURE MANAGEMENT

The loading scheme chosen relies on some method of keeping a constant differential pressure referenced to a variable chamber pressure. Allowance must be made for leakage anywhere in the system for thermal expansion of gas.

The pressure management system is shown in Figure 3. The numerous valves are needed to bleed and fill the system, zero the transducer, and permit optimum operation of the control system. The differential pressure transducer senses the loading piston pressure with respect to the high pressure chamber. Control electronics operate low limit and high limit solenoid valves to keep the differential pressure at the desired level. This level is set by a pressure setpoint with an associated deadband control. The electronic circuitry is shown in Figure 4. Provision has been made for an auto-zeroing solenoid which would be installed in the pressure transducer. This feature would be necessary for long term unattended tests to account for thermal drifts. The accumulator in the loading piston loop reduces oscillations in solenoid switching.

The lowest pressure limited part of the system is the Sealol type 676 AGT-TBK000-16 tungsten-carbide face seal. As mentioned, it is rated up to 300 psi. The rest of the system will withstand at least 500 psi. All metal parts which will operate at low temperatures are austenitic stainless steels, 6061 aluminum, or copper. These materials do not become brittle at low temperatures. A port has been placed at the very top of the pressure chamber to allow "hydrotesting". This has not been done and is recommended before any high pressure testing. A clean non-corrosive fluid such as methyl alcohol should be used.

---

* Feurlon C is a polyimide material manufactured by Rogers Corporation, Connecticut.

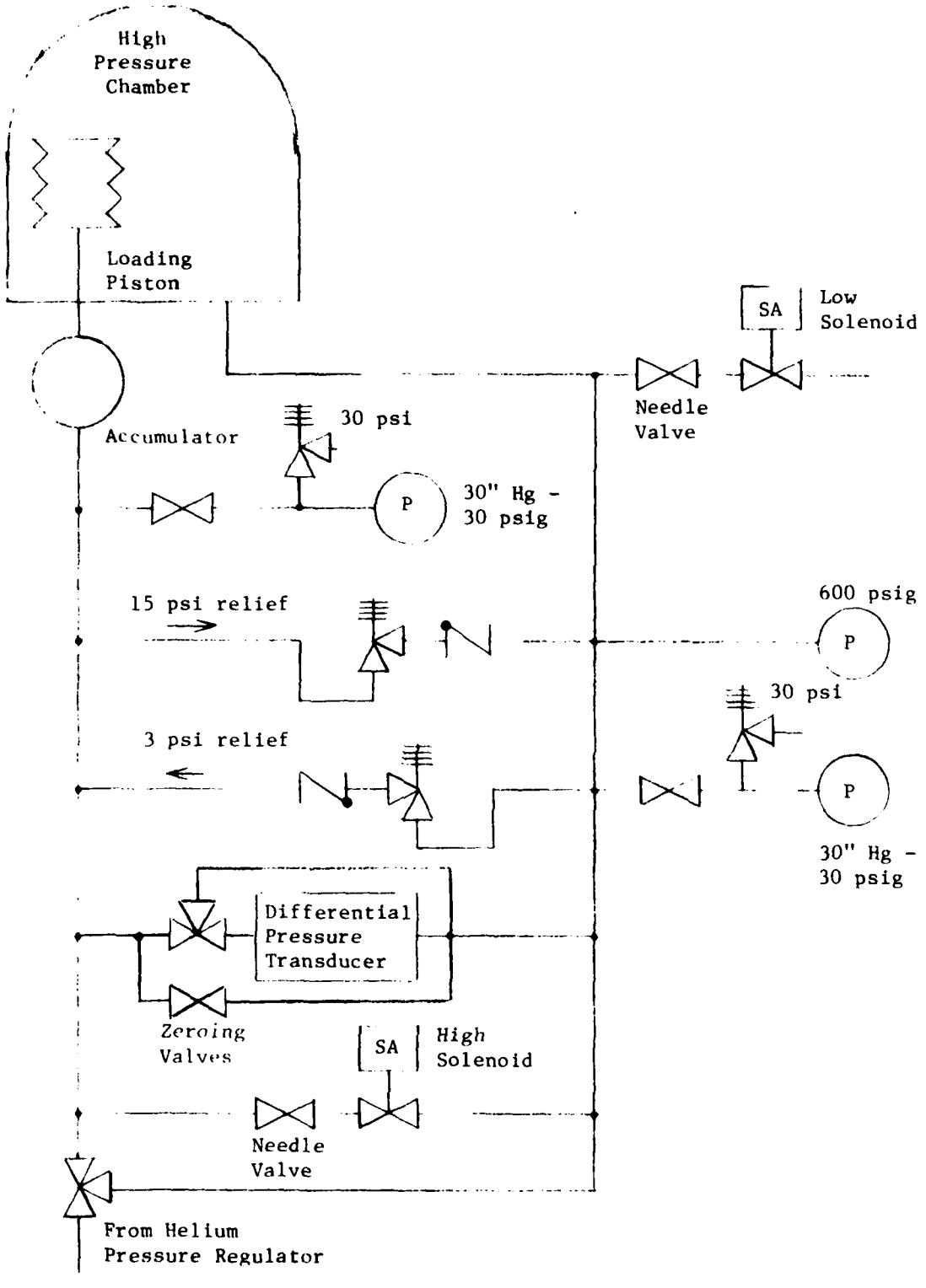

Figure 3. Pressure Control System

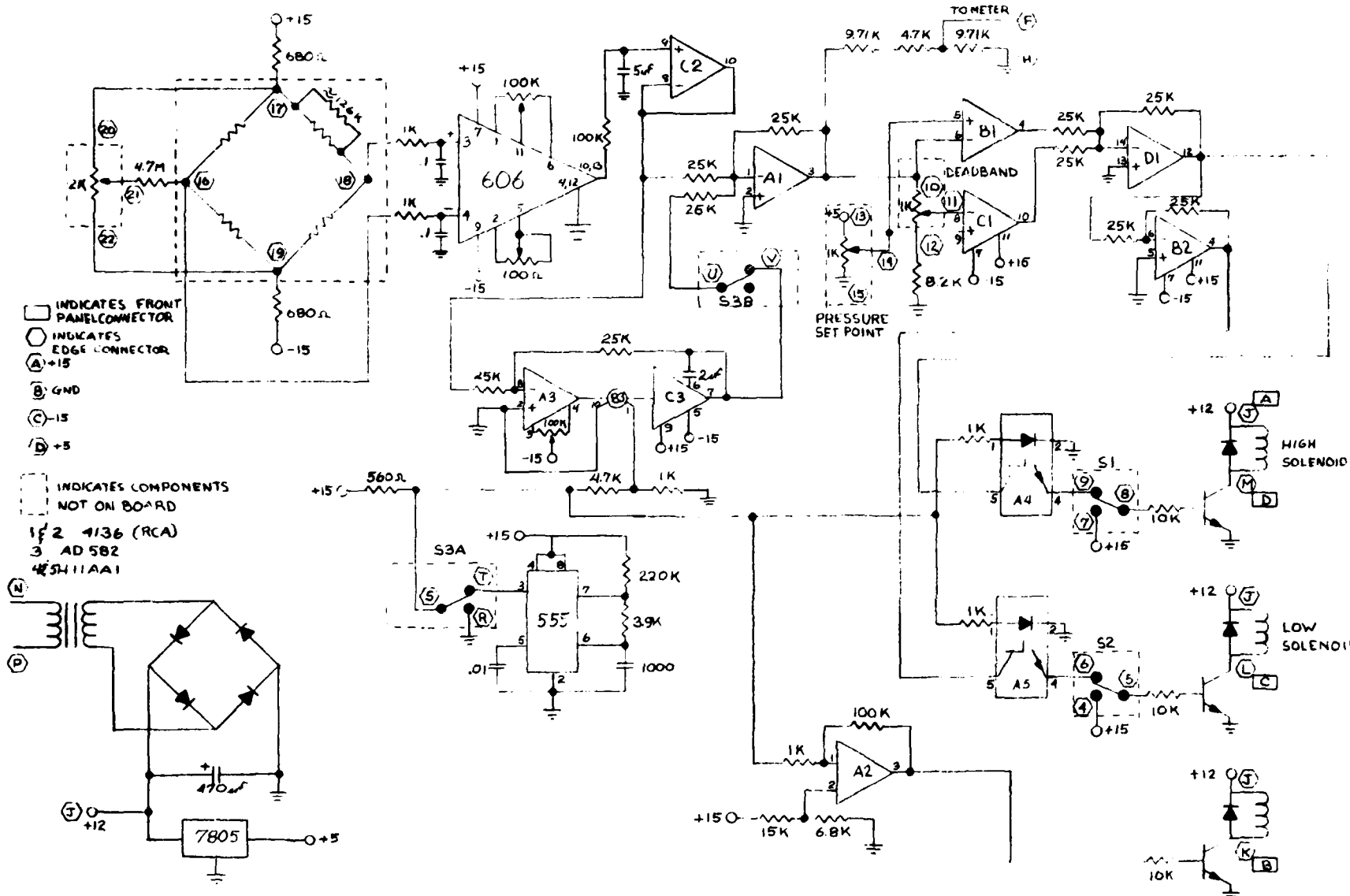

Figure 4. Auto-Zeroing Pressure Control

There are numerous 300 series stainless steel threaded fasteners in the system. In order to prevent galling between mating parts, "Vacuum Goop" (trade name, Crawford Fitting Company) was used as a thread lubricant. It is sold specifically for that purpose.

For room temperature tests, removable components such as the pressure cap and fittings could be sealed with standard elastomeric O-rings. However, at colder temperatures elastomeric seals become ineffective and must be replaced with metal seals. Metal O-rings can be used and all parts which do not have to be disassembled have these installed. Indium foil seals are used for some of the differential pressure seals on the transducer loading beam.

Because of the expense of using a new metal O-ring on the pressure cap each time, it may be desirable to use a silver brazed ring of soft copper wire for the seal. The thermal expansion coefficients for copper and 304 stainless steel are almost identical, and the slight difference (9.2 ppm/^{o}F for copper and 9.6 ppm for 304) would tend to tighten the ring at lower than assembly temperatures. A hertz stress calculation shows that only 60 pounds of vertical load on the copper ring would plastically deform it. The load applied on the sealing ring by the cap bolts can exceed 20,000 pounds. The bolts can be torqued to greater than 100 foot•pounds if care is taken to transmit no large forces to the support legs. For low pressure room temperature tests with a buna N seal, four bolts evenly spaced and tightened to 20 foot pounds are sufficient.

To maintain a pressure tight seal over a wide temperature range some bolted members have been specially designed. Stainless steel bolts with special 17-7 ph spacers were used to bolt the aluminum loading beam to the cold head junction block. The stainless bolts and spacers have a combined thermal expansion coefficient equal to that of aluminum.

A sliding joint is used to seal the cold head to the vacuum system. It is designed to allow movement between the CRYODYNE drive unit and its cold stage which results from thermal expansion. The sliding seal operates at approximately room temperature as do all vacuum baseplate seals.

A standard vacuum valve is used to connect the roughing pump to the vacuum baseplate inlet. A second vacuum valve modified for high pressure use connects the roughing pump to the high pressure system.

3. TRANSDUCER DESIGN

A friction and wear test apparatus must provide a means for measuring the friction force during sliding. The normal specimen load must also be known in order to calculate a friction coefficient and a wear rate.

It is often possible to utilize a dead weight load and eliminate measuring the normal load. However, this was not desirable for a number of reasons. For one, an electrical signal corresponding to the normal load can be used to compute the friction coefficient. This involves dividing the friction force signal by the normal force signal in an analog divider (Figure 5). A continuous output results which automatically takes into account variations in normal load due to vibration and other factors.

Space constraints also make it difficult to use a simple dead weight normal loading system. Also, the load could not be easily adjusted or removed in a pressurized chamber. In view of this, a pneumatic piston type of loading arrangement was devised which is easily controlled over a wide load range. The load is approximately 0.5 pounds per psi of control pressure. The loading piston is an integral part of the measurement beam and the plate specimen is mounted on it.* Figure 6 shows the general arrangement. The pin specimen reciprocates and the forces on it are not measured directly. Since the forces on the plate equal the forces on the pin, forces can be measured on either member.

The measurement section of the transducer is a symmetric 2-axis beam dynamometer. It is a strain gage device with two 4-arm bridges to independently measure the friction force and the normal force. The dynamometer presently in use is designed to work with loads in the vicinity

---

* Both the piston and the bore are hard-anodized aluminum which have been honed for a close fit. The piston is bellows sealed, and in operation, it does not move appreciably for a constant normal load.

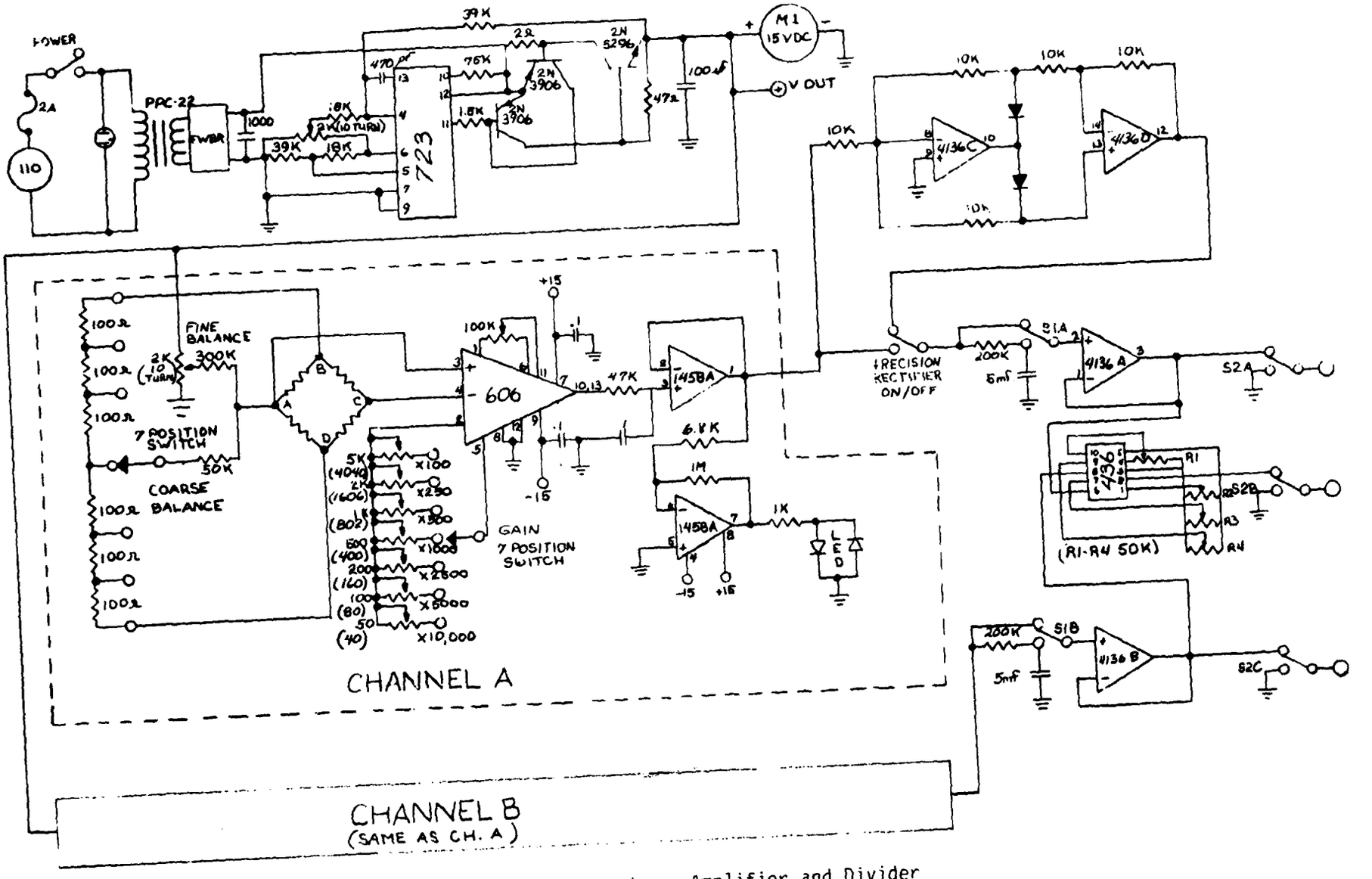

Figure 5. Transducer Amplifier and Divider

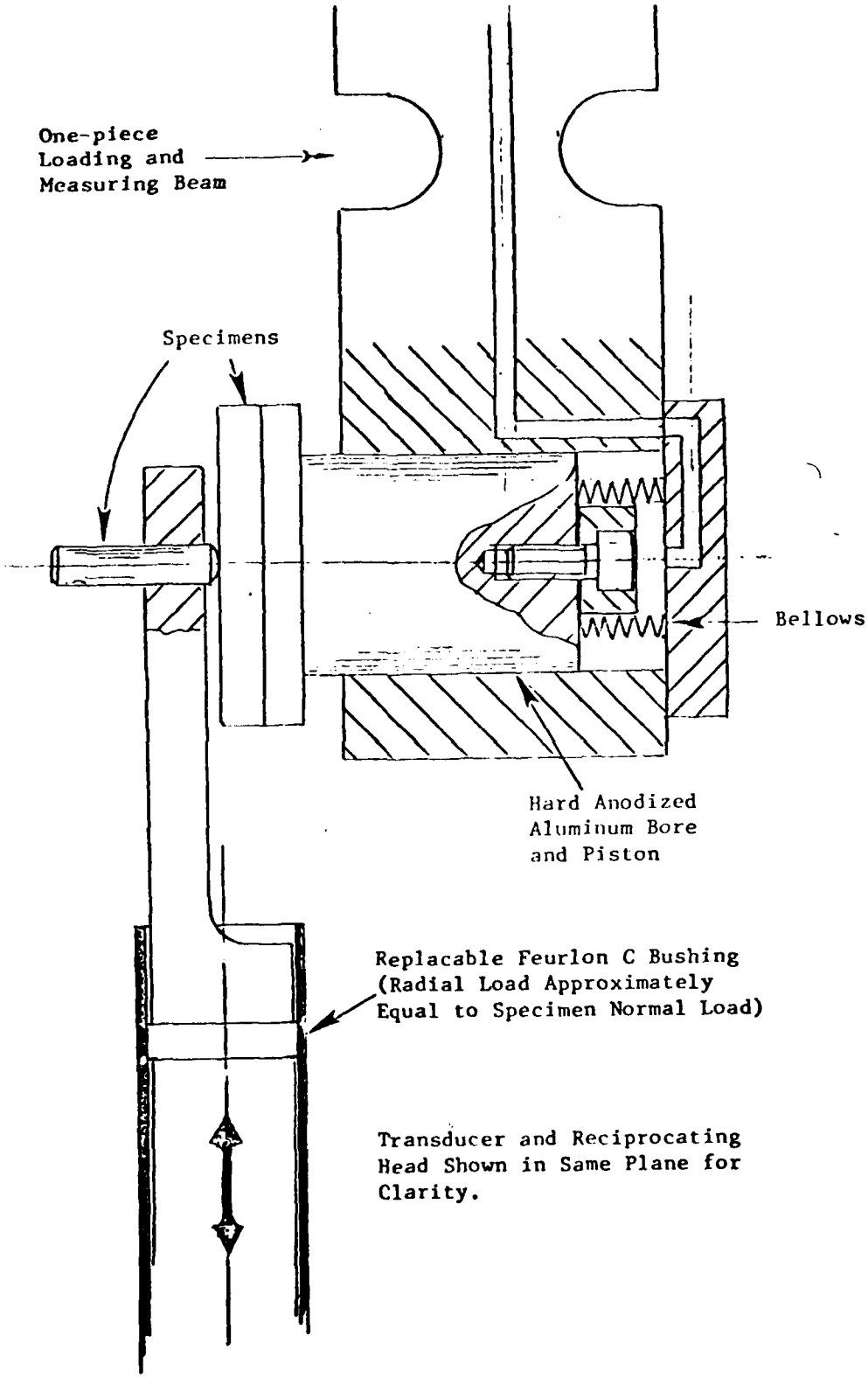

Figure 6. New Specimen Loading Arrangement

of one pound. It will also work up to tens of pounds with the present control system.

Originally, a beam dynamometer was designed and built which was instrumented with semiconductor strain gages. These gages had a zero temperature coefficient of gage factor which would give the dynamometer a force sensitivity which would be independent of temperature. Problems with mounting semiconductor gages led to the use of standard wire foil gages with a reduction in design sensitivity. This reduction permitted its use at loads of 10 pounds but at lower loads it was not satisfactory. The main reason for using semiconductor gages was to provide a high thermal conductivity path from the specimen to the cold head. A large measuring beam cross section was possible if semiconductor gages were used. This was especially important at high normal loads because of the large amount of frictional heat generated. Keeping the temperature drop across the strain gage section below $10^{o}C$ was difficult at 10 pounds of normal load. At 2 pounds of normal load, less heat is generated and a smaller beam cross section is acceptable.

The following are design equations for the present two-axis beam transducer.

Strain at measurement point

$$\epsilon = \frac{6\ PL}{Ebh^2}$$

$$V_{out} = V_{in} \times \text{Gage Factor} \times \epsilon \times \text{gain}$$

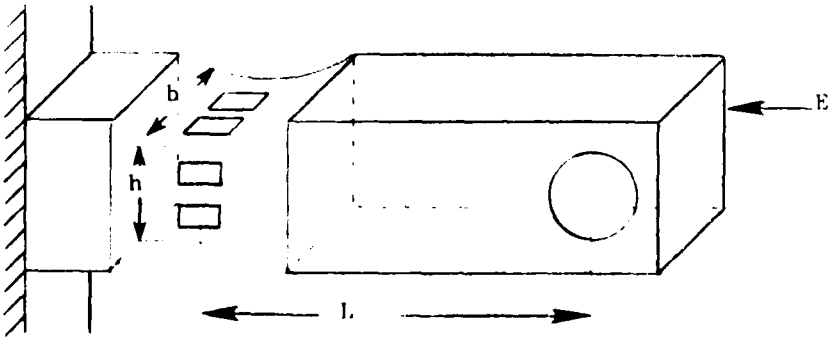

STRAIN MEASUREMENT SECTION

where

G.F. = 2.145, wire foil gages, Micro Measurements type CEA-13-062UW-350

V_{in} = 10.00 volts, bridge excitation

Gain = 2500 typical, maximum available from amplifier is 10,000

b = 0.628"

h = 0.628"

L = 2.717"

E = 10×10^6 psi - 6061 T6 Aluminum

which for 1 pound of load gives a theoretical calibration of 14.5 μV/V/lb. Actual calibration with dead weight loads gives an output of 15.69 μV/V/lb ±1% on both channels. Theoretical and actual calibrations correlate to within 10 percent.

Theoretically, if all the gages are at the same temperature the bridge will remain balanced regardless of its absolute temperature. However, small variations in operating temperature between gages could produce some electrical offset which would require rebalancing with no test forces on the transducer. For this reason, an easily removable normal specimen load is necessary. Optimally, this load removal is performed during a test without more than a few seconds of test interruption. Manual operation of either the high solenoid or the interconnect valve will remove the normal load. In either case, the low solenoid should be disabled.

4. THERMAL DESIGN

Cooling can be provided by a CRYODYNE (CTI Model 1020) low temperature refrigeration unit. The CRYODYNE can provide 22 watts of cooling at 33°K. The maximum cooling capacity at room temperature is about 55 watts. As a secondary means for cooling, liquid nitrogen can be run through coils brazed to a copper junction block located between the CRYODYNE cold head and the dynamometer base. Copper-constantan thermocouples will monitor the temperature of the stainless steel pressure vessel baseplate and the temperature of the copper specimen mounting plate. Cartridge heaters are located

in the baseplate to rapidly bring the system to room temperature after conducting a low temperature test.

An overall thermal analysis of the friction and wear apparatus involves 3 basic parts:

A) Determine heat load on test chamber
B) Estimate cooldown time
C) Calculate steady-state test specimen temperature

PART A -- HEAT LOAD ON TEST CHAMBER

1) Radiation from cold chamber to environment.

Assume infinite gray surfaces with emissivity ϵ equal to 0.1. N radiation shields can be placed in the space between the cold chamber and the bell jar. Aluminized mylar wrapped around the cold chamber with any gap between layers is sufficient.

$$q = A_1 F \sigma (T_A^4 - T_S^4)$$

$$T_S = \sqrt[4]{\frac{N T_A^4 + T_C^4}{N + 1}}$$

$$F = \frac{1}{\frac{1}{\epsilon_A} + \frac{1}{\epsilon_2} - 1}$$

with N = 4 the resulting radiation nest load is 1 watt.

2) Conduction through support legs (3).

$$q = \frac{KA\,\Delta T}{L}$$

1" OD tubing, 0.035" wall

$A = 7.37 \times 10^{-4}$ ft^2

q = 2.15 watts for 3 legs

3) Conduction through supply lines, same equation as in 2).

1/4" helium line	0.18 watt
3/8" transducer wire line	0.38 watt
1" vacuum line	1.40 watts

4) Convection in supply lines.

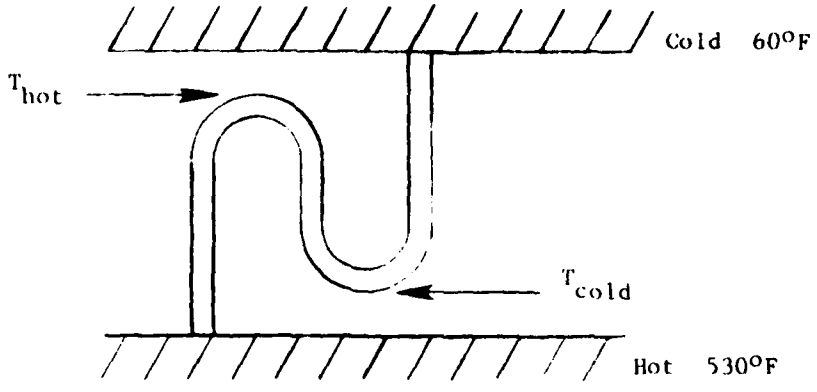

Convection is stopped by the heat trap design depicted above.

5) Conduction down drive tube and containment tube.

Containment tube	0.77 watt
Drive tube	0.53 watt

The drive tube is filled with fiberfrax insulating material and then evacuated and sealed to eliminate convection.

6) Shuttle loss due to reciprocating drive rod in containment tube.

$$Q_{SH} = \frac{0.186\ S^2\ \pi D_C K_g\ \Delta T}{g\ L}$$

$$= 1.2 \text{ watts}$$

7) Conduction through vacuum.

Through a perfect vacuum conduction would be zero. However, the conduction through a moderate vacuum is not well defined in the case of a system likely to be partially filled with helium at various temperatures. It is safe to say that if the vacuum is lower than 0.1 micron the conduction mechanism is free molecular, and if the vacuum is greater than 100 microns the conduction is a continuum similar to room pressure gas. The intermediate region is a transition region. In the free molecular region, the heat load would be less than 1/2 watt at 33°K for the present system (assumes 2.5 ft^2 of surface). In a continuum, 50 watts would be an approximate value, and the transition region would be somewhere in between. Fifty watts is excessive, and an estimated necessary vacuum for 10 watts of heat load might be 1 micron. This is on the order of the lowest pressure obtainable with a roughing pump with no cryopumping. Cryopumping will occur in the test apparatus but not for helium. With no helium, the roughing pump with the cryodyne could get to 0.1 micron. This is not likely to be the case, and some experimentation will be necessary to determine the steps necessary to obtain an acceptable vacuum. A diffusion pump could be added to remove helium, but hopefully it would not be necessary.

8) Pumping loss due to reciprocating motion.

A heat-trapped return line is provided to eliminate gas flow in the drive tube gap. The return line connects the bottom of the reciprocating shaft to the top of the shaft with a very low fluid resistance path. An additional benefit is a large reduction in pressure pulsations which would result due to the reciprocating drive tube's motion.

PART B -- ESTIMATE OF COOLDOWN TIME

The minimum cooldown time can be roughly estimated from the specific heat C_p of the mass to be cooled down. There is roughly 60 pounds of stainless steel, 4 lbs of aluminum, and 5 lbs of copper which would be cooled 300°C. With appropriate values of C_p, 1 kilowatt hour of energy has to be removed. This is without any other heat loads. Since the cryogenic cooler has at most 55 watts of cooling capacity, the cooldown time would be greater than 24 hours. In order to reduce this time an auxiliary liquid nitrogen boiler has been added. With 25 lbs of LN_2, the cooldown time to 77°K should be approximately 1 hour. For a more rapid cooldown, the boiler located between the cold head and the chamber base would have to be redesigned. Actual total cooldown time to 33°K will depend strongly upon heat loads.

PART C -- STEADY-STATE SPECIMEN TEMPERATURE

The steady-state test specimen temperature can be calculated assuming a value of heat generation and a transducer base temperature. At 2 lbs of normal load, a friction coefficient of 0.5, and 3.8 1" strokes per second, approximately 0.86 watt will be generated. The ΔT through a typical sample would be 2°C, and the path to the cold head would have a 1°C drop. Specimen - chamber radiation would reduce the ΔT even further so the operating temperature would be only a few degrees higher than the cold head temperature. Both the chamber base and the specimen mounting platform have copper-constantan thermocouples installed.

SECTION VI
TEST PROCEDURE

1. OBJECTIVE

The purpose of the screening tests was to examine a large number of candidate ceramic materials for their friction and wear characteristics. All materials should be tested once for a preliminary screening and many should then be tested again for a longer time period. Only preliminary screening was performed in this program. Materials found to be comparatively poor in wear resistance would then be eliminated from the more extensive testing to be performed later.

2. SAMPLE PREPARATION

All screening tests were reciprocating pin-on-plate tests. The ends of all the pin specimens were ground to a 1/4" radius. Both the spherical end of the pin and the plate were ground to a surface finish of 10-20 μin. This was done to eliminate the surface finish variable in comparative testing.

The pin and the plate were ultrasonically cleaned twice in clean trichloroethene for 15 minutes, spray degreased with trichloroethene and then baked at 100°C for 12 hours. After cooling to room temperature, the specimens were weighed to 0.01 mg on an analytical balance and mounted in the test apparatus.

3. PRELIMINARY SCREENING

After the specimens were mounted, the high pressure chamber was sealed and the system evacuated to the limit of the roughing pump. This vacuum was held for 1/2 hour and then 15 psig of helium (99.995 purity) was admitted. The system was then pumped down again for 1/2 hour and again 15 psig of helium was put into the system. The specimens were loaded to test conditions and the reciprocating mechanism turned on for 60 minutes. After this period,

the chamber was depressurized and unbolted and the specimens removed. They were visually examined and weighed for weight loss and subsequent wear rate determination.

A nominal 2 pound test load was used for all tests. Although it is likely that the wear rate will be a linear function of load, there are some possible wear mechanisms in which the wear rate varies as a higher power of load. Because of this possibility, a constant load was used for all screening tests. The wear rate should be measurable in a one-hour period, but if it is too rapid the wear mechanism present may not simulate that mechanism in the cryogenic cooler.

On a theoretical basis, a hertz contact stress can be calculated for a loaded pin on disc surface. This calculated stress should be lower than the hardness of the material in order to eliminate yielding or plastic deformation. The hertz stress is:

$$\sigma = 0.388 \quad 3\sqrt{\frac{PE^2}{R^2}}$$

where

σ = compressive contact stress, psi
P = pin load, pounds
E = Young's Modulus, psi
R = pin radius, inches

σ for a 2-pound test load and 1/4" radius pin averages 125,000 psi for typical test materials. This stress is much lower than the stress necessary to provide plastic deformation in an indentation hardness test. For this reason, 2 pounds does not seem excessive for test purposes. As an example, silicon carbide has a hardness of 4 million psi and is far from being plastically deformed.

4. DATA ACQUISITION

During testing, normal force and friction force were monitored continuously. These forces were used to compute automatically the friction coefficient μ, which is the friction force divided by the normal force. These three variables were displayed on an oscillograph so that the friction coefficient could be correlated with specimen velocity. Sample speed varied from 0 to 30 inches per second as the pin oscillated back and forth across the plate.

Following testing, wear of the pin was measured by weighing on an analytical balance. Because the wear was expected to be very low on the best materials, the amount of wear was also determined by measuring microscopically the size of the wear zone on the spherical pin. This volumetric method gave an effective weight loss when multiplied by the material density.

A consistent method must be used to describe the relative wear rates of the various test materials. The wear rate will be defined to be:

$$W^* = \frac{V}{LX}$$

where

W^* = wear rate, $in.^3/lb \cdot in.$
V = wear volume, $in.^3$
L = normal test load, lbs
X = total distance slid, inches
(time x 2 x peak amplitude x cycles/time)

A wear rate thus defined is useful for actual life calculations in a cryogenic cooler. The reason time is not explicitly included in the wear rate is because it is not time but distance slid which is the relevant factor. Given an experimentally determined W^*, and also an acceptable wear volume and load, the life of the sliding system is determined.

For these experiments the nominal test load was 2 lbs, the nominal test time 60 min, the peak amplitude 1 in, and the cycles/time equaled 3.8/sec.

SECTION VII
TEST RESULTS

Table 3 lists the tribology test results. Hot pressed AlN was tested six times under a number of different test conditions. (As the pin was not refinished between these tests, Table 3 lists the initial wear flat diameter for each test in parentheses.) A significant difference was noted between the wear data collected in room air (atmospheric pressure) and that collected in dry helium. Three tests were run in atmospheric air to assess the repeatability of the measurements. The observed wear data scatter is within a factor of two which can be expected for this type of friction and wear test. The wear for the tests run in dry helium, however, appears to be an order of magnitude larger than the atmospheric tests. In order to determine the cause of the observed differences, a test was also completed in clean, dry air, and the resulting wear had a magnitude of 14.2. There apparently is no significant difference between the wear resulting from an environment of dry air and dry helium, thus implicating moisture as the controlling variable in the observed differences in wear rates.

The volume loss tabulated in Table 3 was calculated from the average diameter of the wear flat on the pin, which was measured with an optical micrometer. The predicted volume loss was calculated from the weight loss of the pin, which was measured on a Mettler balance sensitive to 10^{-5} g. The correlation between the predicted and measured volume losses is better for those materials exhibiting high wear, reflecting mass measurement errors. The HP TiC and Fluorogold mass losses were not measurable due to the low densities and low wear rates observed. The HP TiC appeared to be the best material in wear and second only to Fluorogold in friction coefficient.

Table 4 lists the value of wear (W^*) and the average friction coefficient ($\bar{\mu}$) for the Si_3N_4, SiC, and Al_2O_3 materials.

TABLE 3

WPAFB TRIBOLOGY TEST RESULTS - ROOM TEMPERATURE, 1 HR

Rank	Chart #	Materials	Average Wear Dia. (in.)	Net Volume Lost ($in.^3$)	Mean Load (lb)	w^* $\left(\frac{in.^3}{in.-lb}\right)$ E-10	m Weight Loss (lb)	m/ρ Volume Loss Predicted ($in.^3$)	$\bar{\mu}$	S.D. μ	Chamber Pressure (psig)
	1	AlN	.107 (.103)	.37 E-5	2.00	.68	N/A	N/A	.76	.02	(52%RH) Air
11	2	AlN	.126 (.085)	.403E-4	2.16	6.8	N/A	N/A	.82	.02	17.0 He
	3	AlN	.073 (.040)	.489E-5	1.90	.94	N/A	N/A	.73	.03	(65%RH) Air
	4	AlN	.085 (.073)	.484E-5	2.00	.88	N/A	N/A	.72	.02	(65%RH) Air
	5	AlN	.157 (.126)	.724E-4	1.87	14.	N/A	N/A	.73	.03	Clean Dry Air
11	6	AlN	.1205	.422E-4	2.05	7.5	4.4E-6	.39E-4	.72	.02	15.8 He
	7	A479			1.96		1.1E-7	.80E-6	1.0	.06	15.0
3	8	A473	.0686	.436E-5	1.96	.81	7.3E-7	.56E-5	.79	.03	14.5
17	9	AED	.1467	.936E-4	1.92	18.	7.1E-6	.82E-4	.77	.03	15.3
8	10	B_4C	.0781	.737E-5	2.02	1.3	2.9E-7	.32 E-5	.64	.05	15.4
4	11	EC412	.0731	.564E-5	2.07	.99	7.7E-7	.70 E-5	.69	.02	15.7
9	12	EC422	.0863	.110E-4	1.96	2.1	1.6E-6	.14 E-4	.52	.21	14.5
15	13	K162B	.1431	.845E-4	2.11	15.	1.0E-5	.47E-4	.63	.09	15.0
12	14	NC132	.1230	.458E-4	1.8	9.3	3.8E-6	.32 E-4	.56	.04	15.6
7	15	NC203	.0741	.611E-5	2.01	1.1	9.9E-7	.85 E-5	.60	.05	12-15
5	16	NC435	.0730	.560E-5	2.05	.99	4.8E-7	.44 E-5	.67	.02	15.0
14	17	NbC-TaC-C	.1314	.599E-4	1.98	11.	1.2E-5		.51	.20	15.4
18	18	Pyroceram	.1809	.220E-3	2.13	38.	9.8E-6	.11 E-3	.64	.05	15.0
10	19	Sialon	.1037	.231E-4	1.99	4.2	2.1E-6		.74	.03	14.9
16	20	SN220	.1428	.839E-4	2.02	15.	7.8E-6	.65 E-4	1.0	.05	15.0
1	21	HP TiC	.0384	.425E-6	1.94	.08	Not Measurable		.23	.01	15.4
6	22	NC203	.0746	.611E-5	2.00	1.1	3.3E-7	.29E-5	.63	.03	15.0
13	23	NC132	.1292	.560E-4	1.93	11.	5.6E-6	.48E-4	.80	.04	15.0
	24	Fluorogold	.068	.422E-5		.77	Not Measurable		.13	.02	16.0
	25	Fluorogold	.057	.208E-5	1.97	.39	Not Measurable		.14	.02	15.5
17		AED	.150	.103E-3	1.92	20.			.76	.04	15.0

1-5) Parentheses indicate initial diameter
7) On Al_2O_3-TiO_2
Pin wore through plate coating. μ was constant throughout test.
12) Severe Frictional Oscillations
17) Severe Friction drop, μ_{ss} final = .36
18) Wear Diameter Not Flat; use measure weight loss to predict W*.
22) On NC435
23) On A473
24) On 321 stainless steel
25) On 321 stainless steel

TABLE 4

FRICTION AND WEAR DATA FOR Si_3N_4, SiC, AND Al_2O_3 MATERIALS

Material	W* (10^{-10}) (in^3/in-lb)	$\bar{\mu}$	Designation	Fabrication Method
Si_3N_4	18.	0.77	AED	RS
Si_3N_4	15.	1.0	SN220	S
Si_3N_4	11.	0.56	NC132	HP
SiC	1.1	0.60	NC203	HP
SiC-Si	0.99	0.67	NC435	RS
SiC	0.99	0.69	EC412	RS
SiC	2.1	0.52	EC422	S
Al_2O_3	7.3	0.79	A473	S
Al_2O_3	1.1	1.0	A479	S

The SiC materials appear to be quite similar in friction and wear, an unexpected result since the NC203 is hot pressed and should consequentially be more fully dense and homogeneous than the reaction sintered SiC materials. No information regarding residual porosity or % of theoretical density was available for the NTK materials (EC412, EC422) although the NC435 is reported to be 96.6% dense (Table 3). Large frictional oscillations were noted for the EC422 SiC as evident in the relatively large value of the standard deviation for μ (0.21, Table 3). In general, the SiC materials were acoustically noisier than other materials, and this phenomenon is apparent from the larger variation in friction force.

The Si_3N_4 materials exhibited greater wear than the SiC, perhaps due to the SiC being a somewhat harder material (SiC - 3000 Knoop; Si_3N_4 - 2670 Knoop). The friction coefficients for the Si_3N_4 materials appear to differ significantly, although the statistical confidence level has not been established.

If one examines the values of $\bar{\mu}$ for those materials tested more than once in helium (AlN, AED, Fluorogold - Table 3), one notes a much smaller scatter than that observed for the wear data. Table 5 summarizes these data:

TABLE 5

REPEATABILITY OF FRICTION AND WEAR DATA

Material	W* (10^{-10}) (in^3/in-lb)	$\bar{\mu}$
AED Si_3N_4	18.	0.77
AED Si_3N_4	20.	0.76
AlN	6.8	0.82
AlN	7.5	0.72
Fluorogold	0.77	0.13
Fluorogold	0.39	0.14

The two Kyocera Al_2O_3 materials appear to vary significantly in wear (Table 4) although it is not clear why.

The Los Alamos material (NbC-TaC-C) contains free graphite, although this addition does not appear to aid in lowering the friction coefficient or wear in a dry environment (Table 3). The friction coefficient fluctuated significantly, dropping from an average value of 0.51 to 0.36 at the end of the hour test. These friction variations may be due to the pullout of the graphite.

The test with the plasma-sprayed Al_2O_3-T_iO_2 material failed when the A479 (Al_2O_3) pin wore through the coating on the plate. It is questionable whether the coating that was applied gave a true indication of the material's characteristics. One of the pins that was coated was observed to be chipped and the material appeared to be extremely porous.

SECTION VIII
CONCLUSIONS AND FUTURE CONSIDERATIONS

The use of pin-on-disc tribology tests for the screening of ceramic materials has been shown to be a valid method of empirically selecting a material for friction and wear considerations. The data so obtained are repeatable (Table 5).

Few conclusions can be presently drawn as to the best and worst materials. The rank ordering of the wear cannot be directly correlated to the reported values of hardness, fracture toughness, or strength. Additional characterizations must be done to define the grain size, porosity, and hardness to understand which material properties are most important in predicting a material's wear characteristics. Sintering agents, chemical purity, and variations in manufacturing technique play a role in the differences, and so examining one manufacturer's material may not be sufficient for screening purposes.

Additional materials need to be considered. New materials have been recommended for testing. AVCO produces a Al_2O_3-TiC composite which is being used in cutting tools. Chemical Vapor Deposited (CVD) WC and SiC need also to be examined. The Max Planck Institut has been experimenting with an Al_2O_3-ZrO_2•Y_2O_3 and fracture toughness values of 10 are reported[4]. Ceradyne is producing the same material, but the resulting billets do not appear uniform and the material has not lived up to expectations. Once manufacturing techniques have been perfected, this composite might be an interesting choice for cryogenic use. Additionally, plasma deposited materials need more consideration. Ramsey Corporation is currently manufacturing plasma deposited Al_2O_3-TiO_2 piston rings for the Briggs-Stratton engines. The quality of the Perfect Circle Al_2O_3-TiO_2 sample was questionable, as it appeared quite porous, and had chipped in a number of spots.

Most of the data presented herein are for materials wearing against themselves. The optimum wear combination, however, may be comprised of different materials, and material combinations need examination. Previous wear data will have to be utilized when selecting material combinations to keep the number of tests manageable.

SEM analysis of the wear tracks is needed to ascertain the cause of many of the observed phenomena (e.g., the frictional fluctuations in the SiC data).

One-hour tests appear to be sufficient for the screening and rank-ordering of materials; extended testing is needed to obtain valid wear rate data. Under a present DOE contract[16], the wear rate has been shown to approach asymptotically a constant value after approximately 30 minutes of running. The DOE study involves a pin running against a spinning plate which results in different wear mechanics than the reciprocating motion produces, and this surface break-in phenomenon should be further examined.

The wear produced by fluorogold running against stainless steel should be examined at cryogenic temperatures to establish a more realistic baseline for comparisons. The hardness of ceramics should not be greatly affected by cryogenic temperatures although the fracture toughness, particularly in the case of properly heat treated ZrO_2, may increase dramatically[4].

Finally, it is recommended that the repeatability of the wear data be determined statistically by running the same materials a number of times.

REFERENCES

1. B.R. Lawn, "Partial Cone Crack Formation in a Brittle Material Loaded with a Sliding Spherical Indenter", Proc. Roy. Soc. Land, A 299, 307 (1967).

2. E. Rabinowicz, "Friction and Wear of Materials", John Wiley & Sons, Inc., 1965.

3. D. Scott, Wear of Ceramic Materials, Wear, Vol. 24, 1973.

4. Rowland Cannon, Professor, Ceramics, MIT; personal communication.

5. B.R. Lawn and T.R. Wilshaw, "Indentation Fracture: Principles and Applications", J. Mat. Sci., 10, 1049 (1975).

6. B.R. Lawn and D.B. Marshall, "Indentation Fracture and Strength Degradation in Ceramics", - Fracture Mechanics of Ceramics, Vol. 3, ed., R.C. Bradt, D.P.H. Hasselman, and F.F. Lange, Plenum Press, (1978).

7. A.G. Evans and T.R. Wilshaw, "Quasi-Plastic Solid Particle Damage in Brittle Materials: I Observations and Analysis", Acts Met, 24, 939 (1976).

8. D.J. Godfrey, "The Use of Ceramics in High Temperature Engineering", Metals and Materials, Vol. 2, No. 10 (1968), pp. 305-311.

9. J.C. Sikra, J.E. Krysiak, P.R. Eklund, R. Ruh, "Friction and Wear Characteristics of Selected Ceramics", Bulletin of the American Ceramic Society, Vol. 53, No. 8 (1974), pp. 581-582.

10. D.J. Godfrey, "Ceramics for High Temperature Engineering", Proceedings of British Ceramic Society, No. 22 (June 1973), pp. 1-22.

11. D.J. Godfrey and N.L. Parr, "Consideration of the Possible Use of Refractory Ceramic Materials for Advanced Combustion Chamber Design", Published in "Combustion in Advanced Gas Turbine Propulsion System", I.E. Smith, ed., London, Pergamon Press, 1968, pp. 379-397.

12. D.J. Godfrey, "Silicon Nitride Ceramics for Engineering Applications", Society of Automotive Engineers paper No. 740238, February 1974.

13. Walter D. Syniuta, President, Advanced Mechanical Technology, Inc.; personal communication.

14. "Piston Ring and Cylinder Liner Materials and Lubrication Achievements", Technical Memorandum No. 63, (October 17, 1975), Contract No. EPA-68-04-0004.

15. Harold McCormick, Chief Engineer, Ramsey Corporation; personal communication.

16. DOE Contract No. DE-AC19-80BC10362, "Evaluation of Improved Materials for Stationary Diesel Engines Operating on Residual and Coal-Based Fuels".

APPENDIX
MAGNETIC LINEAR DRIVE DESIGN

The design of the motor is shown in Figure A.1. The derived force equation can be shown to be:

$$F_m = \frac{L_o}{d}\left[(i_1^2 - i_2^2) - (i_1^2 + 4i_1i_2 + i_2^2)\frac{x}{d}\right] \qquad (A\text{-}1)$$

where:

$$L_o = \frac{\mu_o \pi r N^2 d}{2g} \text{ , henries} \qquad (A\text{-}2)$$

and

μ_o is the permeability of free space, 4×10^{-7}

All dimensions are in meters and currents are in amperes.

The motor has the following specifications:

r = 0.1905 m (0.75")
d = 0.01905 m (0.75")
g = 0.00127 m (0.05")
coil length = 0.0281 m (1.50")
plunger length = 0.1524 m (6")
N = 300 turns

If

$i_1 = A + B \sin wt$ and

$i_2 = A - B \sin wt$

the resulting magnetic force F_m is

$$F_m = \frac{L_o}{d}\left[4AB \sin wt - (-2B^2 \sin^2 wt + 6A^2)\frac{x}{d}\right]$$

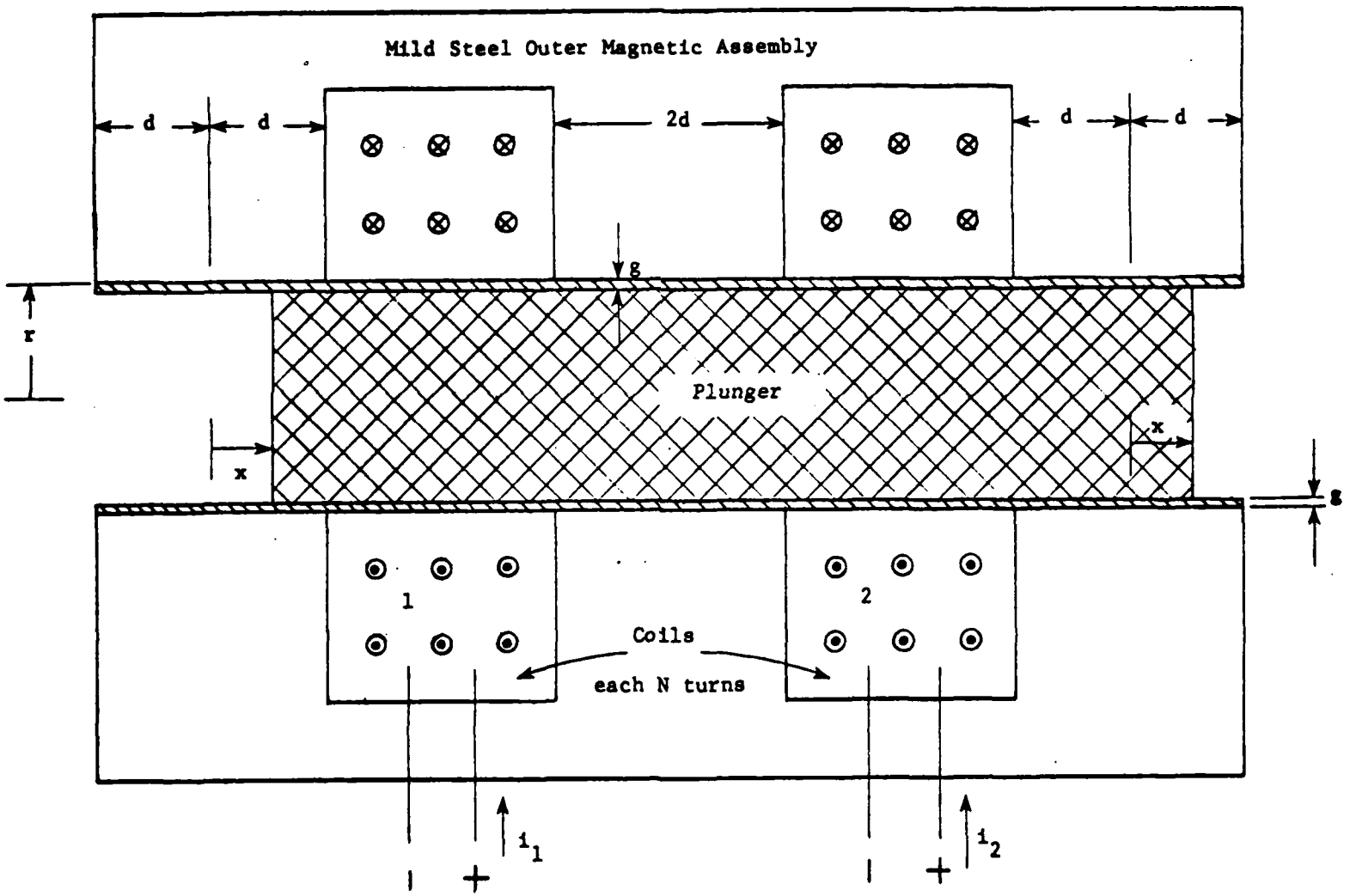

Figure A.1 Magnetic Linear Motor

If no force were necessary to move the magnetic plunger, the resulting displacement could be found by setting F_m equal to 0 and solving for x as a function of time. A curve of such an x for A=B is shown in Figure A.2. It is possible to account for the acceleration force necessary to move the plunger and a friction force which will exist due to the test, but analytically the result is quite complicated. It is perhaps best done by computer. However, the force developed by the motor should be on the order of 5 times greater than acceleration and frictional forces encountered. While these forces will affect the output displacement, an acceptable stroke should still result.

The force developed by the motor is limited by the magnetic saturation of the plunger and solenoid material. This limit sets the maximum useful current, which in this case is about 13.5 amps for a B field of 2 Tesla.

A rotational locking force is applied to the plunger as a result of the cross-sectional geometry shown in Figure A.3. The cutaway sections make the plunger similar to the rotor of a motor with a non-rotating field surrounding it. The currents i_1 and i_2 previously indicated were chosen to provide a net DC level of rotational locking force independent of plunger position. The locking torque T_L is approximately:

$$T_L \cong \frac{B^2 \, g \, l \, (r+0.5g)}{o} = 8.5 \text{ newton meters (75 in.-lbs)}$$

for the dimensions and current levels which will be used.

It would seem to be desirable to close a feedback loop around the linear motor which would give a very specific stroke independent of loading and friction. In practice this is difficult to do in a straightforward manner because of the large inductive load of the motor. The amplifier would have to be capable of very large voltage swings at substantial currents. With no feedback, a $\pm$35 volt compliance $\pm$20 amp dual transconductance amplifier suffices. The voltage and power rating of an amplifier for feedback use would have to be much larger. Since the electrical terminal relationships

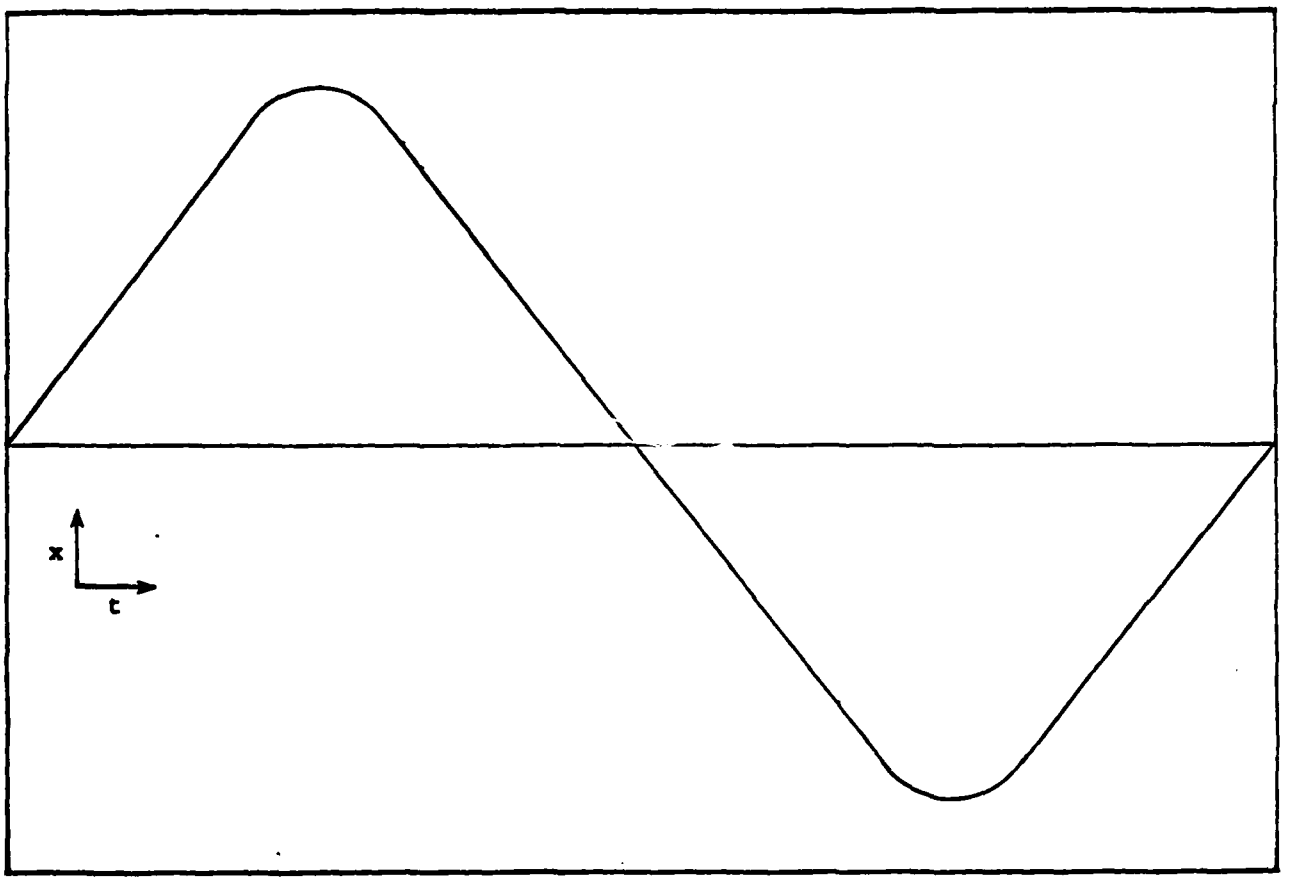

Figure A.2 No Load Displacement Curve for Linear Motor. Period is Equal to Period of Driving Sinusoid.

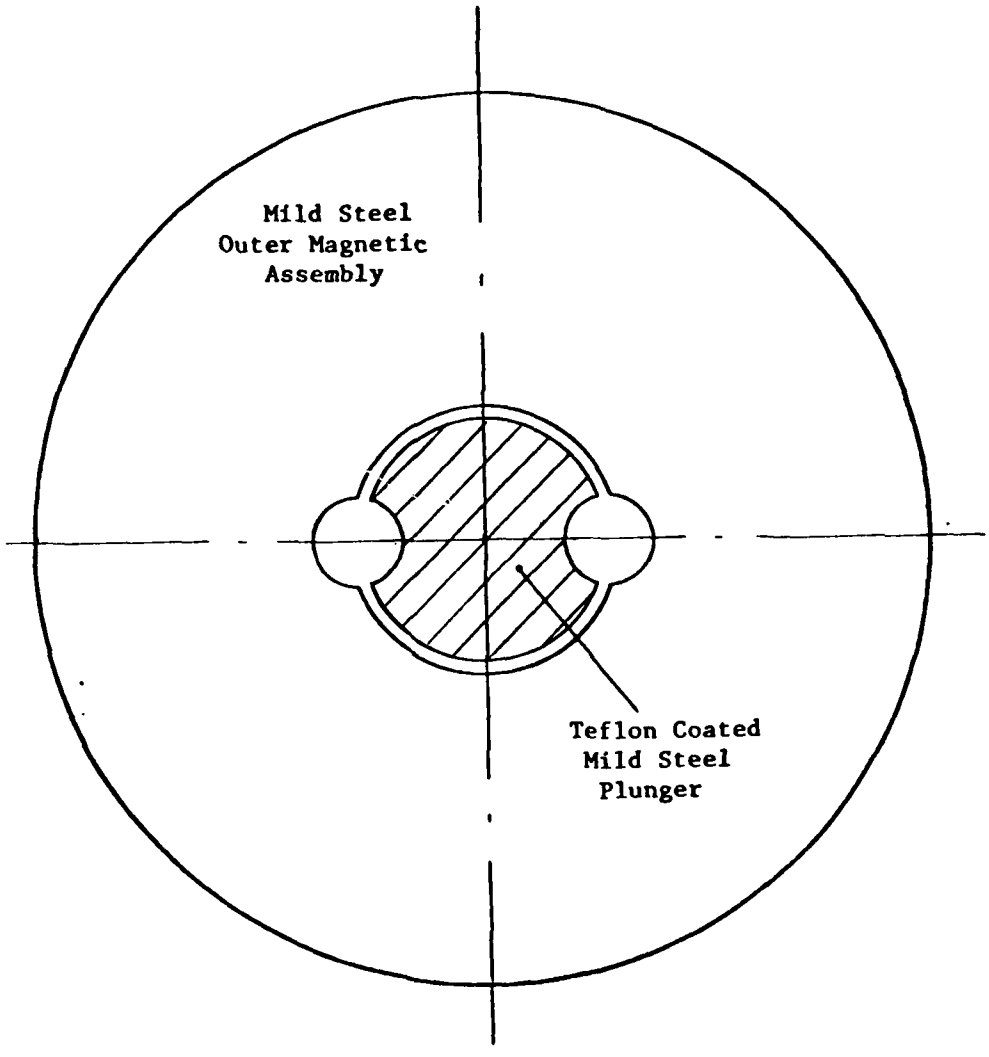

Figure A.3 Cross-Sectional View of Linear Motor Showing Rotational Locking Grooves. A Non-Magnetic Stainless Steel Tube Separates the Plunger and the Outer Assembly.

of the motor vary with both current and displacement, an analytical approach to a feedback model is difficult. Because of the effort and time involved, it was decided to settle for some loading effects and use the stroke which results from open loop operation. The fact that the stroke is not purely sinusoidal should not affect the test results.

In order to monitor the position of the slider, a capacitive displacement transducer was designed. Since the linear motor displacement would be somewhat load sensitive, a means for measuring sliding distance was required.

A general block diagram of the capacitive displacement transducer and associated outputs is shown in Figure A.4. Note that a mechanical counter records actual distance slid independent of stroke or speed. The transducer is constructed of stainless steel and acetal for contamination-free operation. It was never used or completely debugged.

An LVDT or similar device was not used due to fear of contamination from potting compounds or other substances. The presence of strong magnetic fields from the linear motor could also affect an LVDT.

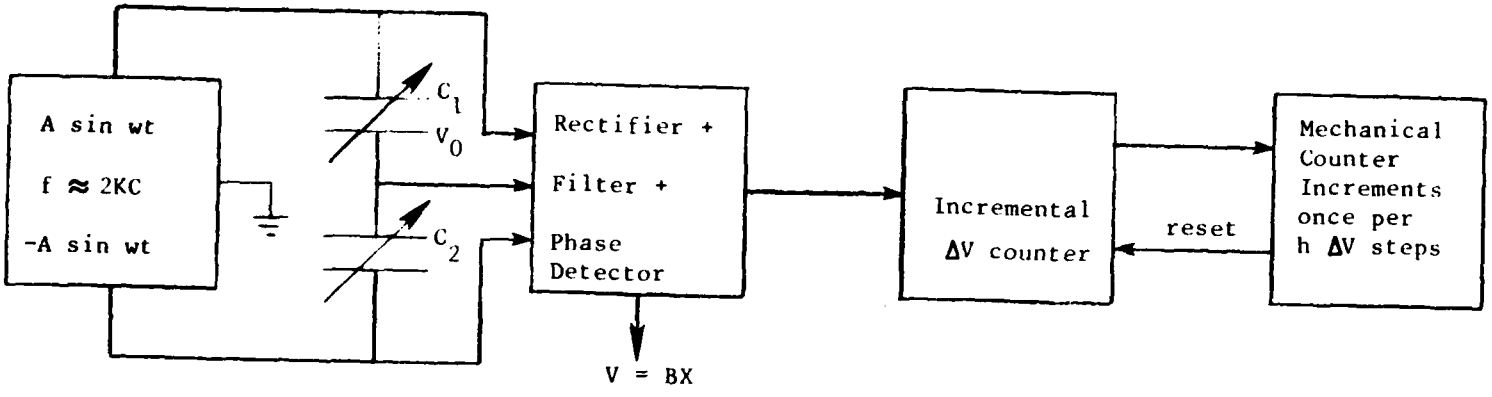

$C_1 = K (L_o + X)$

$C_2 = K (L_o - X)$

$V_0 = A \sin wt \left(\frac{L_o - X}{L_o} - 1 \right)$

X = slider position

A = 10 volts

L_o = 0.75 inch

Figure A.4 Capacitive Displacement Transducer with Sliding Distance Indicator